Cell Reports Methods

CellPress
OPEN ACCESS

Review

Mimicking and analyzing the tumor microenvironment

Roxane Crouigneau,[1,5] Yan-Fang Li,[2,5] Jamie Auxillos,[3,4,5] Eliana Goncalves-Alves,[1,5] Rodolphe Marie,[2,*] Albin Sandelin,[3,4,*] and Stine Falsig Pedersen[1,*]

[1]Section for Cell Biology and Physiology, Department of Biology, University of Copenhagen, Copenhagen, Denmark
[2]Department of Health Technology, Technical University of Denmark, 2800 Kongens Lyngby, Denmark
[3]Section for Computational and RNA Biology, Department of Biology, University of Copenhagen, Copenhagen, Denmark
[4]Biotech Research and Innovation Centre, University of Copenhagen, Copenhagen, Denmark
[5]These authors contributed equally
*Correspondence: rcwm@dtu.dk (R.M.), albin@bio.ku.dk (A.S.), sfpedersen@bio.ku.dk (S.F.P.)
https://doi.org/10.1016/j.crmeth.2024.100866

SUMMARY

The tumor microenvironment (TME) is increasingly appreciated to play a decisive role in cancer development and response to therapy in all solid tumors. Hypoxia, acidosis, high interstitial pressure, nutrient-poor conditions, and high cellular heterogeneity of the TME arise from interactions between cancer cells and their environment. These properties, in turn, play key roles in the aggressiveness and therapy resistance of the disease, through complex reciprocal interactions between the cancer cell genotype and phenotype, and the physicochemical and cellular environment. Understanding this complexity requires the combination of sophisticated cancer models and high-resolution analysis tools. Models must allow both control and analysis of cellular and acellular TME properties, and analyses must be able to capture the complexity at high depth and spatial resolution. Here, we review the advantages and limitations of key models and methods in order to guide further TME research and outline future challenges.

INTRODUCTION

The tumor microenvironment (TME) is a complex, heterogeneous, and spatiotemporally dynamic entity, comprising both cellular and acellular components (Figure 1). Mechanistic insight in the roles of the TME in cancer require *in vivo* and *in vitro* model systems that faithfully reproduce patient TME conditions. The need for such models is illustrated by the numerous failed clinical trials of preclinically promising treatments and the well-documented problems with translating mouse model data to human cancer.[1]

Key roles of the TME in multiple aspects of cancer have been amply demonstrated. TME conditions determine the phenotypic effects of driver mutations, such as KRAS mutations.[2] In patients with colorectal cancer, TME conditions (decreased lymphatic vessel density and reduced immune cytotoxicity) correlated more closely with the risk of metastasis than did key driver mutations or genomic instability[3]; in pancreatic cancer, tumor-associated macrophages (TAMs) produce metabolites that reduce gemcitabine chemotherapy efficacy,[3,4] and the characteristic acidosis and hypoxia within a solid tumor's TME favor cancer cell invasiveness and treatment resistance.[5–7]

Studies using patient tumor biopsies and surgically resected tumor tissue have greatly increased the understanding of how TME properties and biomarkers correlate with disease progression in various cancers.[8,9] Systematic analyses of such specimens can aid treatment decisions, and sequential biopsies before, during, and after treatment can provide insight into treatment effects on the TME.[10,11] Importantly, it is increasingly possible to identify cancer biomarkers and TME biomarkers in liquid biopsies, allowing for less invasive sampling.[12]

Collectively, this poses both challenges and opportunities: it is challenging to include the TME in cancer models, but therapies targeting the TME represent new and potentially game-changing clinical possibilities. Exploiting this requires answers to two key questions: what is the exact TME composition in different cancers and patients and what are the reciprocal links between TME properties and disease phenotype in a given cancer context?

Our ability to obtain these answers is limited mainly by technical challenges: patient samples provide correlative information, and no existing models fully recapitulate the complexity of patient tumor TMEs. Both cancer and stromal cells shape the acellular TME, which in turn impacts all cells within it (Figure 1). These complex reciprocal interactions are highly challenging to dissect in *in vivo* tumors models, whereas simpler models poorly reproduce the *in vivo* situation.

The aim of this review is to present the reader with a critical guide to technical approaches that either are already established techniques for studying the composition and impact of the TME or that, in our view, have the potential to bring such studies beyond the current state of the art. We place particular emphasis on the importance of the physicochemical TME, which has received relatively little attention compared to the cellular TME.

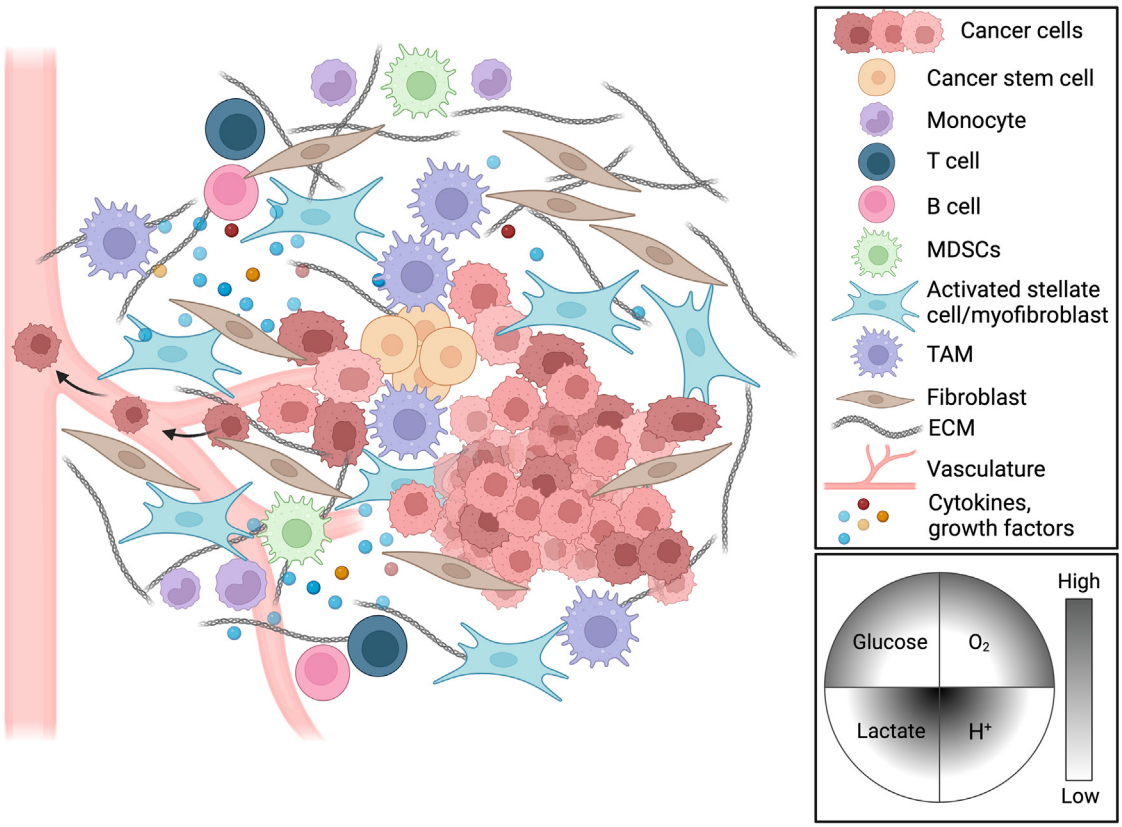

Figure 1. Key stromal and physicochemical components of the TME

Components of the TME favor, as well as restrict, tumor development through paracrine signaling and physical interactions. Growth factors, cytokines, and metabolic waste products secreted by the cancer cells regulate recruitment and function of stromal cells; tumor-associated fibroblasts (TAMs) and stellate cells deposit extracellular matrix; immune cells secrete cytokines and growth factors that suppress or favor tumor growth; and endothelial cells are stimulated by vascular endothelial growth factors (VEGFs) secreted by cancer and stromal cells. Cancer cells entering the vasculature illustrate potentially metastatic cells (black arrows). The top legend shows the stromal components illustrated in the image, and the bottom legend illustrates the 4 major physicochemical TME gradients (gray high, white low). Created with BioRender.

We critically discuss advantages and limitations of these established and emerging models and techniques, ending with recommendations for future work.

THE TME: COMPONENTS, NICHES, AND TARGETING

The cellular TME (Figure 1) varies widely with cancer tissue of origin and tumor-intrinsic factors such as driver mutations. For example, different triple-negative breast cancer subtypes exhibit distinct TME profiles.[13] Cancer-associated fibroblasts (CAFs) as well as multiple classes of innate and adaptive immune cells, which significantly impact disease aggressiveness, comprise the majority of stromal cells in most tumors.[14,15] Depending on the tissue, cancer-associated endothelial cells, stellate cells, and adipocytes are also important parts of the TME[14,16] (Figure 1). Finally, many tumors contain mesenchymal stem cells (MSCs), which are capable of differentiating into multiple stromal cell types.[16,17]

The acellular (physicochemical) TME results from the metabolism, interactions, and secretome of the cells within it and therefore varies with tumor type and spatiotemporally in a given tumor. The physicochemical TME features include extracellular matrix (ECM) composition, architecture, and stiffness[18]; nutrients, metabolites such as glucose, lactate, and fatty acids,[19,20] cytokines, growth factors, and other *bona fide* signaling molecules[21]; exosomes[22]; varying levels of hypoxia, acidosis, and reactive oxygen species (ROS); and fluid and solid pressure.[14]

Substantial spatial and temporal TME heterogeneity has been demonstrated in many cancer types.[23–26] Cancer cells, by virtue of their genomic instability and phenotypic plasticity, can rapidly adapt to, and exploit, local conditions. A well-studied example is the metabolic symbiosis between cancer cells in hypoxic and well-oxygenated tumor regions.[27] Furthermore,[28] antitumor immune cells are inhibited in acidic and lactate-rich regions.[29]

Given the extensive heterogeneity of the TME, its therapeutic exploitation relies on a detailed understanding of the exact TME conditions driving a given cancer cell behavior. For instance, what are the specific combinations of acidosis and hypoxia that drive aggressive behavior in a given cancer, and when are conditions so toxic that even cancer cells cannot survive? How does this balance depend on other cellular and physicochemical conditions? As an example, anti-angiogenic therapy

failed as a single agent, partly because of the resulting hypoxia-exacerbated aggressiveness.[30] Furthermore, degradation of the desmoplastic (dense and fibrous) pancreatic cancer ECM can either improve sensitivity to chemotherapeutic drugs or exacerbate cancer development, depending on the precise context.[31–33] A promising form of TME interference is immuno-oncology approaches that restore anticancer immune response, such as anti-PD-L1/PD or CTLA4 antibodies. However, their success depends on the local TME conditions, such as hypoxia, acidosis, and matrix stiffness.

In summary, the specific TME in a tumor niche can dictate the phenotype of cells within it and play a key role in disease outcome. However, exploiting the TME in anticancer treatment requires that we understand the impact of specific TME conditions and their combinations on cancer cell phenotype.

IN VIVO MODELS FOR STUDYING THE TME

Differences between rodents and humans in the importance of specific TME components for cancer development at least in part underlie the clinical failure of many anticancer drugs that performed excellently in animal models.[34] In this section, we discuss the advantages and drawbacks of different animal models in the context of studying the TME (Figure 2, top).

Mouse models

Since the 1980s, when cell line-derived xenograft (CDX) models were first developed, mouse models of cancer have greatly improved in complexity and ability to simulate human cancers.[34,35] Subcutaneous CDX models remain a central tool in preclinical drug development.[36] However, there is a strikingly low translation from CDX models to patients, with only 3%–5% of developed anticancer drugs eventually approved by the US Food and Drug Administration (FDA),[37] in part reflecting that subcutaneous injection models do not recapitulate the organ TME.[34] Orthotopic tumor models, in which cancer cell lines are inoculated in their organ of origin, allow for a better understanding of how the organ TME impacts drug response and tumor progression but still lack the complexity of the patient tumor.[38] Patient-derived xenografts (PDXs) can better recapitulate the cellular heterogeneity of patient tumors.[39] They can be based on patient-derived organoids (PDOs; PDOs incorporating TME conditions), biopsies, or surgical material directly transplanted, subcutaneously or orthotopically, into immunocompromised mice.[40] PDX models exhibit local TME heterogeneity, histological features, gene expression profiles, and genetic alterations similar to the tumor of origin[41,42] and can predict patient prognosis, as recently shown for pediatric sarcomas.[43] They are, however, not without limitations. To produce sufficient material, PDXs are often serially passaged in mice, where human stroma can be replaced by mouse stromal cells.[44] In addition, they are usually transplanted into immunocompromised mice, resulting in the loss of information about immune cell-cancer cell interactions.[41] This lack of a crucial TME component can be overcome by establishing PDX models in humanized animals such as NOD-SCID *Il2rg*$^{-/-}$ (NSG) mice.[45] Several methods are available for this. Mice can be supplemented with human peripheral blood mononuclear cells (PBMCs), resulting in partial reconstitution of a human immune system dominated by CD3$^+$ T cells. Alternatively, human CD34$^+$ hematopoietic stem cells can be administered intravenously after myelo-ablative irradiation.[46] This model is slower than the PBMC-based model, but recapitulates a more complex immune system, including human CD3$^+$ T cells, CD19$^+$ B cells, and CD14$^+$ monocytes.[47,48] Even more complex models involve the co-transplantation of human fetal bone, liver, and thymus and intravenous injection of CD34$^+$ hematopoietic stem cells, resulting in a diverse human immune system of macrophages, dendritic cells, and T and B cells.[48–50]

Syngeneic mouse models, generated by inoculating mouse cancer cells subcutaneously or orthopically into immunocompetent mice of the same genetic background, overcome some of the disadvantages of CDX and PDX models.[51,52] They do not mimic the cellular heterogeneity of tumors but provide insight into the roles of immune cells, useful, e.g., in evaluating the efficacy of immunotherapy protocols. Chemically induced mouse models are generated by treating immunocompetent mice with carcinogenic compounds. These models have the advantage of including the TME from the organ of origin[53] and can be combined with genetic manipulations.[54] However, it can be challenging to monitor the presence and growth of tumors, and histological subtypes can be very different from those in patients. Finally, genetically engineered mouse models (GEMMs) are generated by mutating or altering the expression of oncogenes in germline cells of immunocompetent mice,[38] resulting in spontaneous tumor formation, mimicking with varying accuracy human tumors arising from similar mutations.[34,55] GEMM-allograft models can be generated from spontaneous GEMM tumors by re-transplantation into animals of the same genetic background, allowing for larger cohorts while maintaining stromal-cancer cell interactions.[55,56]

Mouse models will, to varying degrees, reproduce aspects of the physicochemical TME because the TME, as pointed out above, is a consequence of the activity of the cells in the tumor. It has been demonstrated that tumors contain acidic and hypoxic regions and that tumor interstitial fluid is often high in lactate due to abundant fermentative glycolysis (the TME: components, niches, and targeting).[7,57] However, the precise local physicochemical composition in tumor niches, and how this correlates with the cellular heterogeneity of the tumor, remains understudied. Furthermore, evaluating the causality of a given element of the physicochemical TME in *in vivo* models is challenging because of the complexity of the interactions involved. For instance, inhibiting single TME components, such as ECM re-organization,[58] acidosis,[59] or HIF signaling,[60] is not consistently successful in reducing disease progression.[61,62] This, at least in part, reflects a lack of insight into how reciprocal interactions among TME properties and the cell types in tumors determine the net outcome of such treatments.

Zebrafish models

Over 80% of disease-associated human genes are present in the *Danio rerio* (zebrafish) genome, supporting its use as a human disease model.[63] Zebrafish embryos easily absorb compounds directly from the water, making them valuable models for high-throughput drug screenings.[64] Furthermore, they are optically transparent, and the development of a transparent adult

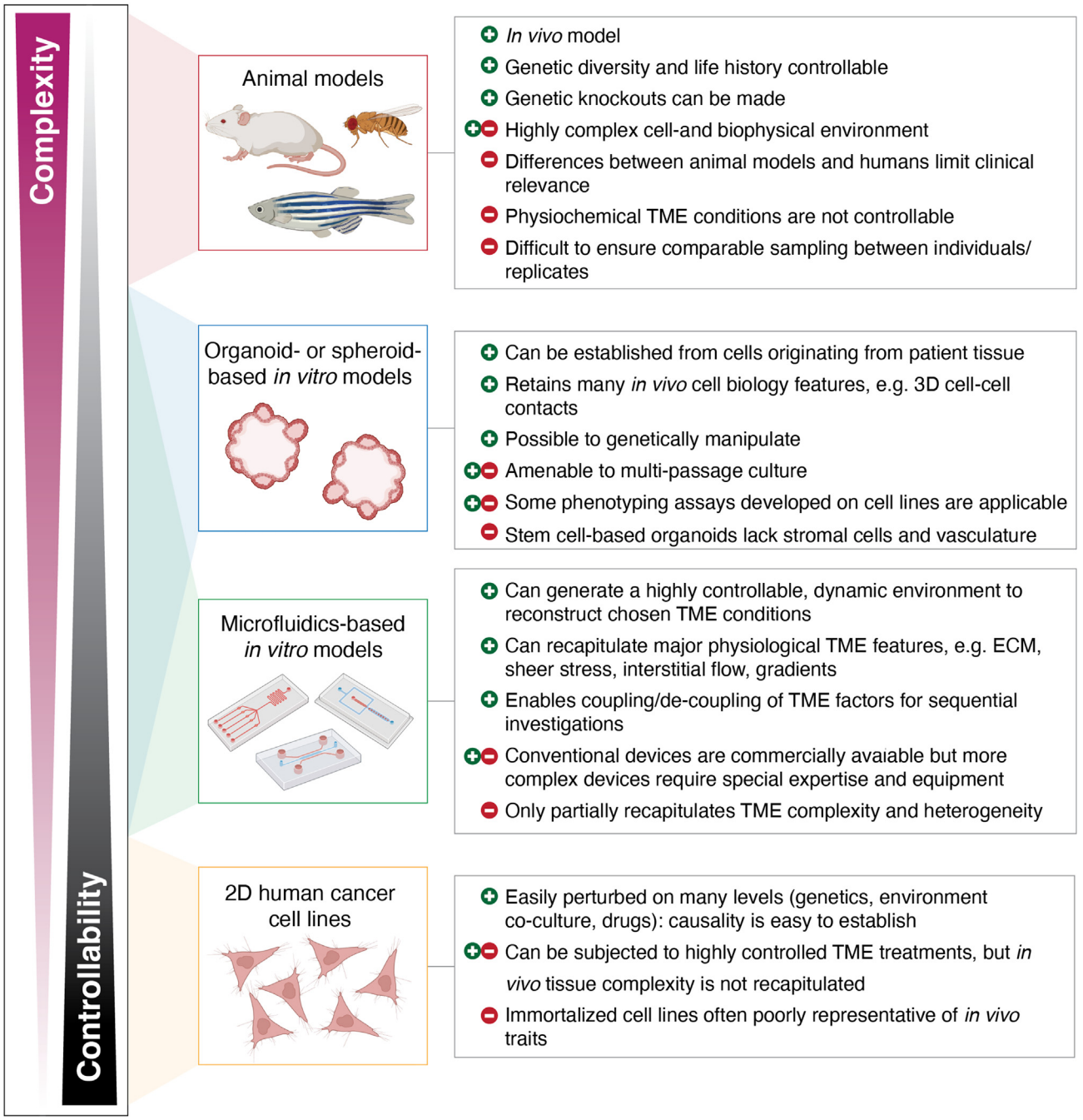

Figure 2. Overview of biological TME models at various levels of complexity

The figure illustrates the main models discussed in the text in order of complexity (top to bottom) and controllability (bottom to top) and summarizes key advantages and limitations of each model. See the main text for details. Created with BioRender and Adobe Illustrator.

zebrafish[65,66] facilitates imaging, e.g., in metastasis studies.[67] Xenograft models can be generated by transplanting human (or mouse) cancer cells or tumors into zebrafish in the embryo or larvae stage, due to the absence of a fully developed immune system.[68] Genetic engineering of zebrafish embryos is less expensive and time consuming than in mice, and a large number of transgenic lines are available, expressing human oncogenes or cell-type-specific drivers labeling nearly all components of the cellular TME for live imaging.[69] Zebrafish models generally recapitulate well histological and genetic features of human tumors, including TME components.[53] On the other hand, zebrafish lack several cancer-relevant human organs (e.g., breast, prostate, lungs), and their immune system is less complex than that of mammals.[34,70]

Models in fruit flies and other non-vertebrates

Strikingly, 90% of the human cancer driver genes in The Cancer Genome Atlas (TCGA) have orthologs in *Drosophila melanogaster*, the common fruit fly.[71] Importantly, while Drosophila lack an adaptive immune system, they have a well-developed innate immune system enabling studies of immune cell-cancer cell interactions. Drosophila models have been widely used to study cancer genetics and have been successfully applied to study interactions between tumor cells and their TME, as well as with more distant organs and systemic physiology.[72] For instance, Drosophila carrying GFP-labeled malignant *RasV12scrib*$^{-/-}$ eye imaginal disc tumors were used to show how cancer cells obtain nutrients by inducing autophagy in the surrounding TME and distant tissues.[73] Recently, similar findings were reported in a Drosophila intestinal tumor model.[74] The *RasV12scrib*$^{-/-}$ eye imaginal disc model has also been used to interrogate interactions between tumors and the Drosophila phagocytes.[75] Finally, both fruit flies and other non-vertebrate model organisms have been used to study cancer cell motility driven by microenvironmental cues.[76]

In summary, *in vivo* models of widely varying complexity can provide valuable information about the cellular and acellular TMEs and their impact on cancer development. However, for dissecting causal interactions between TME elements, these models are not ideally suited because of the difficulty in controlling TME conditions *in vivo*.

IN VITRO MODELS INCORPORATING TME CONDITIONS

Numerous cancer studies, including otherwise sophisticated approaches such as complex CRISPR screens, are still carried out on cell lines in two-dimensional (2D) culture in plastic dishes, completely ignoring the TME. Not surprisingly, and consistent with the ability of 3D cancer cell spheroids to recapitulate many TME properties,[77,78] CRISPR screens carried out in 3D spheroids are superior to 2D screens in identifying cancer-relevant targets.[79,80]

2D *in vitro* models (Figure 2, bottom) employing controlled changes in the one or more elements of the physicochemical (hypoxia, pH, ECM) or cellular (endothelial cells, immune cells, fibroblasts) TME conditions do, however, have the advantage of enabling tight control of such parameters and have contributed important information on, e.g., genetic cancer drivers.

Today, incorporation of TME conditions in *in vitro* cancer models is increasingly enabled by the development of advanced hydrogels,[81] tumor-derived ECMs,[81,82] and other biomaterials for complex cell culture and novel techniques such as microfluidics (microfluidics-based methods for mimicking and analyzing the TME). In the following, we focus on how TME conditions can be included in organoid-based cancer models (Figure 2, second row from top).

General properties of organoid-based tumor models

Organoids are 3D multicellular structures comprising both differentiated cells and stem cells, which can divide indefinitely and genetically resemble their tissue of origin.[83,84] Since their first description in 2009,[83] stem cell-derived organoids have been generated from a wide range of tissues from model animals and humans and have gained particular attention in cancer research. Depending on the culture conditions, tumor organoids may comprise only epithelial cells or stromal cells and ECM components.[77,83,85] The various approaches and their advantages and limitations are discussed in the following section, using PDOs as the example.

PDOs incorporating TME conditions

Organoids generated from patient tumor tissue (PDOs) are widely used and can be obtained from publicly available repositories.[86] Today, PDOs can be generated even from diagnostic fine-needle biopsies,[87] allowing, in principle, *in vitro* screening of tumor drug response during the short time window from diagnosis until treatment must be initiated.

A clear advantage of PDOs over traditional cell cultures is their closer resemblance to the patient tumor. Mouse orthotopic PDXs generated from PDOs can be used for *in vivo* validation of drug response, and organoids can again be cultured from the xenograft tumors (mouse models). Using bladder cancer PDOs, such organoid models were shown to maintain a high degree of heterogeneity and clonal evolution in culture and mimic the chemotherapy response of both patient tumors and PDX mouse models.[88]

A potential limitation of cancer organoid models is that depending on the culture approach, they may or may not reflect the cellular TME. In submerged Matrigel cultures of organoids, where only epithelial cells are maintained, stromal TME components can be introduced by co-culture with multipotent progenitor cells[89] or individual stromal components. For example, vascularization can, to some extent, be introduced by co-culture with vascular organoids (forming so-called assembloids), terminally differentiated endothelial cells, or multipotent progenitors.[90] To study tumor cell-immune cell interactions, different classes of immune cells can be isolated based on human PBMCs from the same patients and co-cultured with their organoids, as in a recent study of PDOs from patients with gastric cancer.[91] Variations of this include shaking cultures of Matrigel-embedded organoids, in which patient glioma-derived PDOs were shown to recapitulate both tumor-like stem cell distribution and tumor physicochemical conditions such as hypoxia gradients.[92] Alternatively, culturing PDOs using the so-called air-liquid interface (ALI) method enables preservation of endogenous stromal components. For example, the ALI method was shown to preserve both CAF and T cell function in PDOs derived from melanomas, lung cancer, and renal cancer,[93] and cytotoxicity assays of co-cultures of rectal cancer PDOs with patient-matched tumor-infiltrating lymphocytes predicted the response to neoadjuvant chemoradiotherapy and anti-PD-1 antibodies.[94] Recent work combined patient-derived cancer cells, CAFs, and immune cells in Matrigel ECM to patient-matched organotypic co-cultures, which retained key features of patient tumors better than the cancer cells alone.[95] Similarly, single-cell sequencing of patient-derived glioblastoma (GBM) models showed that patient tumor similarity was strongly enhanced by combination with human embryonic stem cell-derived cerebral organoids.[96]

In summary, PDO models are superior to cell culture models in mimicking human tumor traits. However, also in such models,

care must be taken to retain and/or reconstruct cellular and acellular components of the TME.

MICROFLUIDICS-BASED METHODS FOR MIMICKING AND ANALYZING THE TME

Microfluidics-based methods are powerful tools for TME modeling *in vitro* (Figure 2, third image). They are characterized by sub-mm dimensions enabling laminar flow, which makes it possible to (1) expose cells to temporal variations of chemical conditions with minimal mixing; (2) control fluid flow-induced shear stress at length scales ranging from μm to mm to recapitulate the flow conditions in blood and lymph vessel and interstitium; (3) remove accumulation of waste products; and (4) establish chemical gradients perpendicular to the flow by balancing flow velocity and diffusion coefficients.[97] In recent years, the "entry barrier" for non-specialists to use microfluidics devices has been lowered by the availability of commercial platforms for less specialized applications (e.g., Mimetas, Ibidi, Elveflow, Dolomite) and on-demand microfluidic chip fabrication services. However, because of the complexity of the TME, most studies of this topic remain dependent on homemade devices with dedicated designs.[98–100]

Microfluidic mimicking of the physicochemical TME

Tumor interstitial fluid flow has laminar characteristics,[101] which are mimicked in most microfluidic studies of cancer cells.[102–106] Two main device designs are used: tumor cells are either seeded in a channel flanked by two flow channels delivering growth medium, with interstitial flow generated by offsetting the pressure in the channels,[104,105] or the cell-seeding channel is also used to deliver the growth medium.[102,103,106] A few studies have combined blood, lymph, and interstitial flow, based on a design using a cell-seeding channel flanked by two channels to generate interstitial flow, one of which is used as a "blood vessel" and the other as a "lymph vessel."[107,108] The pressures in the three channels are adjusted to mimic typical values of pressure and flow velocities in the blood flow, lymph flow, and interstitial flow *in vivo* (Figure 3A).

Mechanical stress is a fundamental feature of the TME and plays a crucial role in tumor progression and cancer treatment.[111,112] Such stress can originate from the pressure of the liquid, referred to as the interstitial fluid pressure (IFP) and may include hydrostatic and osmotic pressure, and/or ECM deformation or other solid mechanical forces, in which case it is also referred to as solid stress.[113,114] In microfluidic models, liquid pressure is easily adjusted by, for example, adjusting liquid height in the medium reservoirs leading to a hydrostatic pressure[102,104,108,115] (Figure 3G). Osmotic pressure, stemming in large part from the attraction of cations to negatively charged glycosaminoglycans in the ECM,[116] can be mimicked by applying medium with altered ionic strength[116,117] (Figure 3H). IFP can be emulated alone by imposing pressure onto the fluid in the absence of flow (Figure 3G); however, to the best of our knowledge, existing studies (e.g., Lee et al.[107]) have only mimicked IFP combined with interstitial flow (Figure 3A). Solid stress can be imposed independently of flow conditions in microfluidic devices made of flexible material and/or including moving parts[109] (Figures 3B and 3C) and can be combined with fluid pressure as, e.g., in a study on lung function,[118] but is equally relevant for TME studies.

In contrast to essentially all other models, microfluidics can be used to accurately and reproducibly mimic and analyze the spatiotemporally heterogeneous chemical environments in the TME by generating concentration gradients that are either imposed on cells or arise from tumor cell metabolism inside the device. Key such gradients include pH,[110,119] oxygen,[110,120,121] growth factors,[119] nutrients,[110] and cytokines.[122,123] The chemical composition of the medium can be modulated temporally so that the same cells are sequentially exposed to different conditions (Figure 3E).[110,121] Alternatively, cells are exposed to different chemical environments simultaneously in parallel on the same microfluidic device.[124] Most interestingly, microfluidics allows the creation of a chemical gradient over a cell culture, thus reproducing chemical gradients on the length scale of a tumor of interest (~100 μm to mm).[119,123]

Microfluidic mimicking of the cellular TME

In recent years, microfluidics has been used to mimic aspects of the cellular TME of a wide variety of cancer types, stromal cells, matrices, and flow conditions.[125–128] Because of the rapid advances in, and potential of, combining PDOs with microfluidics, this will be our focus in the following. As described in the section in vitro models incorporating TME conditions, PDOs can faithfully mimic many aspects of patient tumors; however, they are generally low throughput, and most PDO culture methods reproduce only in a limited way the complex TME. To address such limitations, recent work has integrated PDOs with microfluidics, ranging from relatively simple growth of organoids in droplet microfluidics[129] to organ-on-chip technologies.[130,131] To design an organ-on-chip system, key features of the target organ, such as cell types, structural organization, and physicochemical microenvironments, are reproduced. The devices often contain multiple, individual microchambers to grow multiple cell types while controlling the environment in a cell-type-specific manner. The devices are produced using microfabrication techniques such as soft lithography.[132] By integrating PDOs with organ-on-a-chip engineering, TME-relevant microenvironments can be generated.[131,133] Examples include a culture system in which patient-derived, triple-negative breast cancer stem cells were developed into cancer organoids in an on-chip system, while TME conditions could be controlled and monitored in real time[134]; the combining of pancreatic cancer PDOs, stellate cells, and macrophages in an organ-on-a-chip microfluidic device, resulting in functional, patient tumor-mimicking TME interactions[135]; the combining of microfluidics to impose microenvironmental pH gradients mimicking those in the TME on breast cancer cells with Visium-based spatial transcriptomic analysis, as recently done by our team[136]; and a model including microfluidics-driven peristalsis to mimic the TME of gastrointestinal tumors.[137]

In summary, by combining cancer and stromal cell types from patients or model systems with microfluidic devices, the cellular and physicochemical aspects of the TME can be integrated into tumor models in a tractable manner. While still simplified compared to *in vivo* models, such models enable controlled

CellPress
OPEN ACCESS

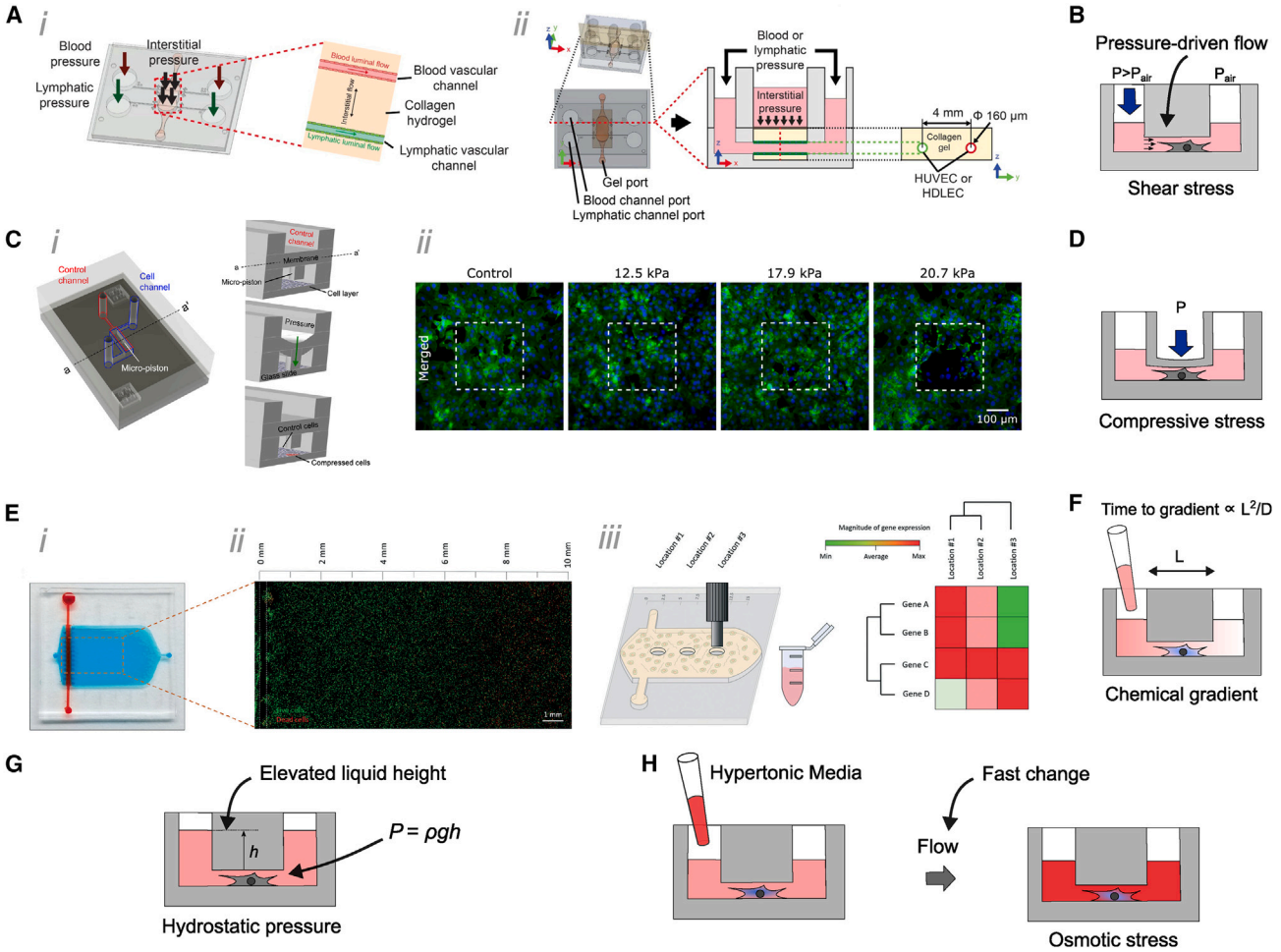

Figure 3. Microfluidic models for mimicking the physicochemical TME

(A) (*i*) Microfluidic device designed to mimic the native transport unit of solid tissues, including a blood vessel, interstitial tissue and ECM, and a lymphatic vessel. The model enabled control of blood, interstitial, and lymphatic pressure through fluidic ports and a central reservoir. Spatial pressure gradients drive luminal flow through the lymphatic microvessel (green arrow) and blood microvessels (red arrow) and interstitial flow through the collagen gel (black arrow); (*ii*) top view of Multi-Flow platform demonstrating port geometry, cross-sectional view of the platform to demonstrate pressure modulation, and orthogonal cross-sectional view of collagen hydrogel and microchannels in which human umbilical vein endothelial cells (HUVECs) are cultured to form the blood vessel and human dermal lymphatic endothelial cells (HDLECs) are cultured to form the lymphatic vessel. (*i*) and (*ii*) are reproduced from Lee et al.[107] under the Creative Commons Attribution 4.0 license. Copyright 2022, IOPscience.

(B) A hydrodynamic flow is created by a difference of pressure *P* applied at the inlet/outlets of a microfluidic device. Hydrodynamic flow is created, associating an elevated pressure and a shear stress on the cells.

(C) (*i*) Assembly design of the chip composed of the control channel (in red) for introducing gas pressure and cell channel (in blue) for cell culture. The concept of applying compression on cells is illustrated by the membrane deflection and micro-piston brought onto the cells by the pressure applied through the control channel and retracted back after compression. Thus, the localized part of the cell monolayer under the micro-piston is compressed, while the rest acts as control (not drawn to scale). (*i*) and (*ii*) are reproduced from Onal et al.[109] under the Creative Commons Attribution 4.0 license. Copyright 2021, Frontiers.

(D) An external pressure *P* applied to a deformable microfluidic device can mimic solid stress applied by the ECM.

(E) (*i*) Picture of the microdevice filled with blue- and red-colored water for visualization purposes. HCT-116 cells were embedded in a collagen hydrogel instead of the blue area; the red area mimics the lumen channel. (*ii*) Confocal image showing HCT-116 cell viability after 24 h in the microdevice at 10 MIO cells/mL. Viable and dead cells are shown in green (calcein-AM [CAM]) and red (propidium iodide [PI]), respectively. White dashed line indicates the lumen position. (*iii*) Scheme illustrating the protocol to retrieve the cells from the device. Both halves are disassembled, exposing the collagen hydrogel, and hydrogel punches are isolated using a biopsy puncher. (*i*)–(*iii*) are reproduced with permission from Ayuso et al.[110] Copyright 2019, The Royal Society of Chemistry.

(F) A steady-state chemical gradient is typically obtained after a time proportional to L^2/D.

(G) A hydrostatic pressure can be applied by the height of the liquid *h* in the inlets and outlets without associated flow.

(H) Osmotic pressure can be created by sequentially introducing hypo- or hypertonic medium.

analyses of the implications of changing specific TME conditions. Furthermore, microfluidic models can be built around fully human cell types, increasing their translational value. Finally, microfluidic models are compatible with a wide range of readouts based on, e.g., live imaging, immunofluorescence (IF) analyses, sequencing, and proteomics, as discussed in the following sections.

LIVE IMAGING OF THE TME

TME imaging in patients with cancer

Clinical imaging techniques are available to probe different features of the TME.[8] Dynamic contrast-enhanced imaging, computed tomography (CT), and magnetic resonance imaging (MRI) can be used to evaluate aspects of the TME, including vascular function, enabling detection of, e.g., lung metastases.[138] Quantification of tumor hypoxia using oxygen contrast or the paramagnetic properties of Hb is well established.[139,140] Tumor fibrosis can be assessed using MRI to monitor water diffusing, tissue stiffness, and fat content, although signals can be confounded by tumor necrosis.[141,142] A wide range of TME properties, including hypoxia, pH, ECM properties, and stromal cells, can be imaged using positron emission tomography (PET).[143] A more recent technique, photoacoustic imaging (PAI), is in clinical trials as a way to visualize the TME based on light pulses, absorption of which by the tissue generates specific ultrasound wave patterns.[144] PAI allows for the imaging of TME features such as vasculature, oxygenation, pH, ECM properties, and lipid composition without the use of contrast agents or radiolabeling agents.[8]

Live TME imaging in preclinical models

In addition to methods in clinical use, as described in TME imaging in patients with cancer, preclinical models can be combined with *in vivo* fluorescent imaging techniques to obtain detailed information regarding TME conditions. Methods include whole-animal fluorescence imaging approaches based on near-infrared (NIR) or two-photon imaging using genetically encoded or injected reporters.[145–147] These techniques allow real-time imaging relatively deep in tissues, making it possible to study biological mechanisms, single-cell behavior, cellular heterogeneity,[146] and immunotherapy efficiency.[145] They can also provide detailed information on aspects of the physicochemical TME, including, for instance, oxidative stress.[148]

EX VIVO SPATIALLY RESOLVED ANALYSES OF THE TME

Multiplexed protein visualization

Dyes such as Sirius red or periodic acid Schiff (PAS) have been used for decades to study tumor ECM properties and antibodies to identify specific proteins. Today, developments in multiplexed analyses have greatly expanded the potential of immunohistochemistry (IHC) for understanding tumor complexity. For instance, the multiplexed cyclic IF method MxIF allows studies of 61 antigens in the same tissue section.[149] Other approaches involve multiplexed ion beam imaging (MIBI) of antibodies tagged with isotopically pure elemental metal reporters[150] and co-detection by indexing (CODEX), in which antibodies are iteratively visualized using DNA barcodes, fluorescent dNTP analogs, and an *in situ* polymerization-based indexing procedure[151]; for other cyclic microscopy methods, see Elhanani et al.[152] Such emerging techniques provide the precision of IHC and similar optical imaging methods but at a scale more suitable for integrated analyses of the TME.

ISH techniques

In situ hybridization (ISH) is a family of methods utilizing labeled probes for the detection of RNA or DNA. Briefly, a set of probes is added to a fixed tissue to hybridize with their target sequence and is subsequently imaged using microscopy. RNAscope is a commercially available ISH-based technology relying on primary, secondary, and tertiary probes, collectively enabling sensitive spatially resolved RNA quantification.[153] Within the context of the TME, RNAscope has been used in diffuse-type gastric cancer to identify an enrichment in CCL2+ endothelial cells and fibroblasts in the deep tumor layers compared to the superficial layers.[153,154] Multiplexed error-robust fluorescence ISH (MERFISH) is a variant of ISH that uses a sequential hybridization and barcoding strategy to increase the number of RNA targets that can be detected.[155] Applying MERFISH to the TME, Hara et al. targeted 135 genes in a patient GBM sample and observed an enrichment of macrophages adjacent to mesenchymal-like GBM cells, with subsequent experiments revealing that macrophages drove the transition of GBM cells into a mesenchymal-like state.[156] The MERSCOPE platform based on MERFISH was recently made commercially available, with premade and customizable probe panels for targeting hundreds of genes.

A limitation of the ISH techniques is that they are restricted to pre-defined probe panels, limiting the range of RNA targets under investigation. The subsequent section describes techniques used to capture biological molecules without the use of predefined panels of probes or antibodies against a subset of DNA, RNA, or proteins.

OMICS TECHNOLOGIES FOR STUDYING TME PROPERTIES

"Omics" techniques, which aim to characterize and quantify large sets of biological molecules (proteomics, genomics, etc.) in a single experiment, have the advantage of being comprehensive and not subject to ascertainment bias, making it possible to find unexpected patterns. We focus on genomics for profiling changes in DNA (genomics for studying the TME), transcriptomics for assessing RNA expression (transcriptomics for studying the TME), and proteomics to measure protein abundance and modifications (proteomics for studying the TME). We will discuss these technologies as applied on three levels of biological material: bulk/tissue, single-cell (sc), and spatial levels (Figure 4). These techniques, especially those with spatial and/or single-cell resolution, have already revolutionized the understanding of the stromal TME. Other spatially resolved techniques, including spatial metabolomics, are also powerful tools for unraveling the complexity of the TME but will not be covered here (for reviews, see Planque et al.[157] and Walsh and Quail[158]).

CellPress
OPEN ACCESS

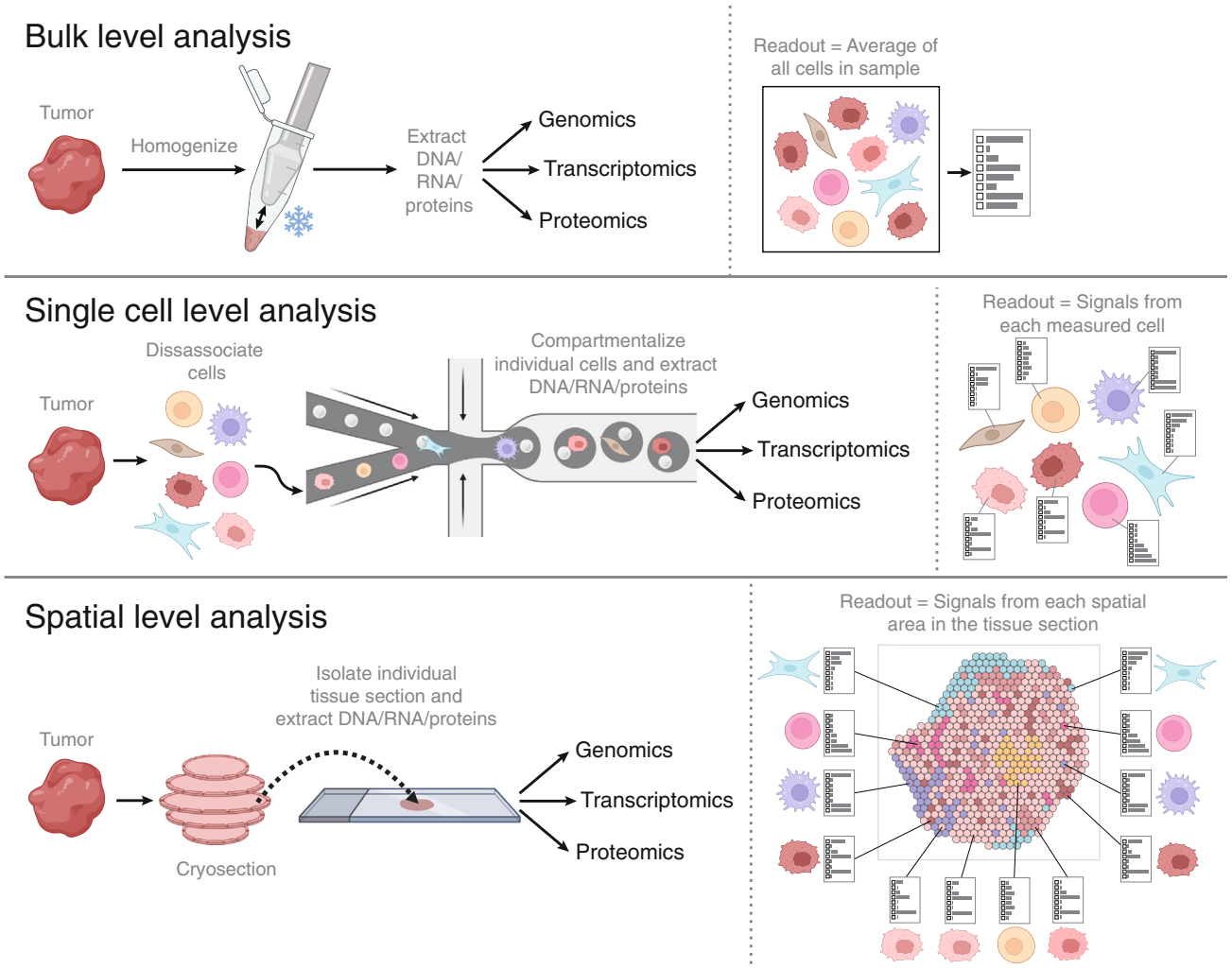

Figure 4. Overview of omics technologies for different levels of biological material for studying the TME

In the bulk level of analysis of tumors (top), the entire tissue is homogenized or pulverized, and the extracted DNA/RNA/proteins are subsequently assessed by bulk omics methods described in the sections genomics for studying the TME, transcriptomics for studying the TME, and proteomics for studying the TME. The resulting readout from a bulk-level analysis is an average of all the cells in the tumor sample. In the single-cell level of analysis (middle), tumor tissue is dissociated into individual cells, which are subsequently compartmentalized and barcoded. DNA/RNA/proteins from each individual cell are analyzed by single-cell omics methods described in the text sections listed above. As each cell is analyzed separately, the resulting signals of DNA/RNA/proteins are obtained for each cell. In spatial-level analysis (bottom), the tissue is embedded and sliced into sections retaining information on the structure of the tumor. A slice of this tumor is placed on a glass slide and subsequently analyzed by spatial omics methods described in the text sections listed above. Resulting signals from this type of analysis can be attributed to different locations within the tumor structure, and depending on the resolution of the omics method used, signals can be attributed to individual cells within the tumor. Created with BioRender and Adobe Illustrator.

Genomics for studying the TME

Genomics is sometimes used as a collective term for molecular biology omics techniques. Here, we use it to refer to the analysis of changes or differences in genomic DNA sequences.

Bulk DNA-seq

DNA sequencing (DNA-seq) analysis can be split into whole-genome sequencing (WGS) and whole-exome sequencing (WES). The latter has been used to great effect to explore driver mutations in diverse cancers,[159] and WGS analysis of 2,658 cancer genomes identified, on average, 4–5 driver mutations per sample.[160] In terms of understanding the impact of local TME conditions, bulk DNA-seq has limited utility because allele frequencies originate from averaging across all cells within the tumor. That said, it is possible to predict clonal cell subpopulations based on allele frequency distributions and thereby assess the genetic heterogeneity of a bulk sample (e.g., as in Andor et al.[161]). Importantly, combining bulk genomics data and additional phenotypes can be used to link the TME with genetic diversity. For example, Sobral et al. showed that tumors from colorectal cancers that were triggered by mutational instability developed heterogeneous microenvironments enriched in immune cells.[162]

Single-cell genomics

DNA-seq of single cells (scDNA-seq[163]) allows characterization of intratumoral heterogeneity on the DNA level. scDNA-seq involves sorting single cells into individual compartments, where they are barcoded prior to sequencing. A key challenge is the necessary step of genome amplification, where biases or errors can be introduced (potential solutions reviewed in Gawad et al.[164]). In a TME setting, the primary strengths of scDNA-seq are (1) identification of co-occurring mutations in a single cell, enabling lineage tracing and assessment of cancer clonal evolution, and (2) if combined with a phenotypic readout, the direct linkage of mutations to cellular phenotype. This is particularly relevant since the physicochemical TME can affect mutation rates, and vice versa, specific genotypes can shape the TME.[7] Despite this opportunity, there are, to our knowledge, no reported studies applying scDNA-seq to explore how mutations in specific subsets of genes are associated with the TME.

Spatial DNA-seq

To study reciprocal TME-cancer cell interactions, it would be beneficial to link the genotype of cells to their location in the tumor. Spatial DNA-seq is still in early phase development. A large challenge is the limited amount of DNA that can be extracted from individual cells, but initial efforts and optimizations have shown some capacity to extract spatial genomics information. A promising technique is slide-DNA-seq, which was used together with spatial RNA-seq (described below) and imaging techniques to relate the spatial localization of cells, clonal identity, gene expression, and a TME component, tumor density.[165]

Transcriptomics for studying the TME

Bulk-level transcriptomics

Bulk sequencing of mRNAs based on fragmentation of RNAs, cDNA conversion, and sequencing of fragments using a short-read sequencer is commonly referred to as "RNA-seq" and is arguably the most mature genomics technique, reviewed in-depth elsewhere.[166] Briefly, RNA-seq reads are mapped to a reference genome or transcript collection to infer gene expression levels, enabling a battery of computational and statistical analysis methods.[167] A new development is methods that sequence intact, full-length transcripts,[168] allowing direct characterization of isoforms, including alternative splicing, at the cost of lower sequencing depth and accuracy. Bulk RNA-seq is most useful when cells display low heterogeneity and have limited spatial information, which, in the context of studying TME impact, makes it the best choice for perturbation studies where cells in culture are exposed to controlled changes of physicochemical environment; see, e.g., Yao et al.[169] The disadvantage of bulk RNA-seq in a TME setting is that gene expression is estimated as an average across all cells in the sample. This can be circumvented if cells are selected based on their TME niche—for instance, by laser capture micro-dissection (LCM) before RNA-seq.

Single-cell-level transcriptomics

scRNA-seq is based on the same methods that underlie bulk RNA-seq, but cells are separated prior to further processing. Incorporation of cell-specific barcodes in the sequenced cDNA enables mixing of all cDNAs from all cells in a single pool, which are sequenced together and computationally separated afterward.[170] A large number of scRNA-seq methods are available, as reviewed in Stuart and Satija.[171] The choice is dictated by sensitivity vs. cell diversity: for example, highly diverse samples, such as complex tissues, require the sequencing of large numbers of cells, at the expense of fewer genes being captured per cell.

While many technical challenges remain, mainly reflecting the lower amount of material per reaction (see Tran et al.[172]), scRNA-seq data allow for a range of analyses not possible with bulk RNA-seq data.[173] These include (1) identifying cell populations with similar expression profiles and quantifying their proportions in the sample, (2) differential expression estimates on single-cell level, and (3) lineage reconstruction, where trajectories across the measured states are predicted. The latter is most meaningful during the transition from one distinct cell type to another[174] or to clonal substructures of tumors (e.g., McCarthy et al.[175]). A somewhat related approach, RNA velocity,[176] uses the ratio between intronic and exonic sequences sequenced to infer the future mature RNA state, making it possible to predict the actual direction of a transition.

scRNA-seq has substantial utility in understanding cellular states in the TME. Examples include studies mostly focusing on cellular heterogeneity of cancer samples, e.g., Wu et al.[177] and Patel et al.[178]; biomarkers for specific disease-relevant cell types within the tumor[179,180]; and TME markers for cancer stages and specific clinical prognosis.[180] Finally, the combination of scRNA-seq with scDNA-seq[181] and assay for transposase-accessible chromatin with sequencing (ATAC-seq)[182] enables further insights at the single-cell level. That said, a major limitation of scRNA-seq in a TME context is that spatial context is lost, making it arguably most relevant for controlled TME changes, or combined with laser capture-dissection of specific tumor regions, as discussed above.

Spatial transcriptomics

A common approach to retaining spatial information is spatial barcoding using immobilized single-stranded polydT oligos containing unique DNA barcodes.[183] A thin tissue section of interest is applied on top of the capture surface(s), and cells are lysed *in situ*. RNAs carrying poly(A) tails (typically mRNAs) from each cell on the section will hybridize to the capture area, followed by cDNA conversion, recovery, and finally short-read sequencing. Computational analysis can de-multiplex the reads, enabling a mapping of gene expression data to spatial locations within the capture surface. Moreover, spatial expression data can be overlaid with images of cell structures, typically by H&E staining of the tissue section. An example of spatial RNA-seq that provided TME information includes Thrane et al.,[184] where a specific gene expression signature in the lymphoid area of melanoma lymph node biopsies, in close proximity to the tumor region, was found. Integration of scRNA-seq with spatial profiling can combine the benefits of both and was used, e.g., in studies demonstrating (1) the localization of a tumor-specific immunosuppressive keratinocyte subpopulation to a fibrovascular niche in human squamous cell carcinoma[185] and (2) the colocalization of stress-responding cancer cells with inflammatory fibroblasts in pancreatic ductal carcinoma.[186]

Finally, it is important to mention the potential of combining multiple sequencing techniques to obtain in-depth spatial

information. As such, the immune cell landscape of prostate tumors was studied by combining scRNA-seq and spatial transcriptomics using the Slide-seq platform.[187] Furthermore, the probe- and imaging-based spatial sequencing platform Xenium was recently combined with scRNA-seq- and Visium-based spatial transcriptomics (both the Xenium and Visium platforms are from 10× Genomics) in an effort to obtain high-resolution information about the cellular heterogeneity of fixed human breast cancer sections.[188]

Proteomics for studying the TME

Proteomics techniques aim to provide a snapshot of cellular/tissue protein repertoire and abundance and, depending on methodology, other molecular features of proteins, such as post-translational modifications. Providing both challenges and opportunities for additional insights, proteins can dynamically localize to multiple intracellular sites as well as in the TME and are modified by post-translational modifications such as phosphorylation. Below, we briefly outline mass spectrometry (MS)-based methods (reviewed in Angel et al.[189]) applicable for studying the TME. MS also underlies lipidomics and metabolomics techniques, which are not covered by this review.

Bulk proteomics

The vast majority of MS-based studies are performed in bulk because single-cell and spatial MS has only recently become feasible. MS can be directly applied to whole tumors; see, e.g., Cao et al.[190] However, while informative, such data are averages across cells and environments.

To explore tumor heterogeneity and TME properties, it is beneficial to couple MS approaches with targeted sampling, e.g., by liquid chromatography of different tumor regions.[191,192] A recent study used proteomics and other genomics methods to characterize regions of pancreatic tumors[193] and found that sub-regions of the TME differed in tumor-promoting and chemoprotection abilities and that stromal heterogeneity could be linked to patient outcome.

The ECM is uniquely targetable by proteomics (reviewed in Hanash and Schliekelman[194]). Of particular relevance to the TME, stable isotope labeling by amino acids in cell culture (SILAC) can identify newly produced ECM constituents and thereby interrogate how tumor cells shape the local TME. Examples include studies of ECM dynamics in hepatocarcinogenesis[195] and ECM composition in pancreatic tumors, separating ECM proteins from cancer and stromal cells.[196]

Single-cell proteomics

Single-cell proteomics is a rapidly developing field, albeit a challenging prospect, primarily because the effective sample concentration is extremely low (reviewed in Labib and Kelley[197]). The current state of the art uses liquid chromatography followed by an MS approach that is similar to many bulk approaches but incorporates multiplexing (e.g., utilizing tandem isobaric mass tagging, exemplified by Li et al.[198]) and boosting prior to the MS step, both aiming to reduce sample loss during preparation. Current single-cell proteomics approaches can quantify around 1,000 proteins per cell. State-of-the-art studies have focused on differentiating macrophages[199] and leukemia stem cells.[200] To our knowledge, single-cell proteomics have not yet directly been used to study TME questions but holds clear promise in this regard, especially during controlled application of specific TME conditions or combined with laser dissection of specific tumor regions, as discussed above.

Spatial proteomics

MS can also be used for spatial imaging (imaging MS, reviewed in Bateman and Conrads[201] and Gessel et al.[202]): a thin tissue slice is coated with a conductive agent, and a matrix promoting peptide desorption and ionization is applied on top of the slide. Desorption and ionization are facilitated by a laser beam applied sequentially across the surface, and ionized peptides in respective locations are analyzed by MS, enabling peptide quantification spatially across the tissue slide.

Although still not a widely used technique, imaging MS holds vast promise for TME studies because of its wide range of applications and targets, including the ability to measure non-proteins, such as drugs. Interesting examples include studies aiming to identify proteins whose expression could distinguish between breast cancer tumor cells and their stroma[203] and to analyze protein diversity in cancer and normal breast tissue ECM.[204] Imaging MS can also be used to assess the penetration of drugs and other treatments in tumors, as shown in a 3D model of malignant pleural mesothelioma.[205]

SUMMARY AND PERSPECTIVES

Whereas the importance of the reciprocal interactions between the TME and the cancer cells within it has been recognized since Paget's famous "seed and soil" theory, the specific composition and roles of the TME in different cancers are still being unraveled. Increasingly sophisticated tools for tackling these tasks have become available in recent years, leading to a surge of new data and models. Patient tumor tissue can now be analyzed at the single-cell and spatial levels, yielding new information about cellular heterogeneity; live patient tumor material can be incorporated into models such as PDOs with integrated stromal components; physicochemical TME conditions can be mimicked using microfluidic approaches; and omics technologies suitable for analysis of the TME are gaining resolution and depth. Importantly, the data from each model and technology represent only one piece of the puzzle, and future breakthroughs in understanding the role of the cellular and acellular TME in cancer development are dependent on combining and integrating these pieces to reveal the full picture. In particular, understanding of the interplay between different TME components and of how interference with individual or multiple components of this complex network can be exploited therapeutically is still very limited, as is knowledge regarding the composition and roles of the TME of metastatic niches. Progress in these key areas will depend on studies combining multiple advanced TME model systems with highly resolved single-cell and spatial analysis methods.

ACKNOWLEDGMENTS

Related work in our laboratories is funded by the Novo Nordisk Foundation (NNF19OC0057739 and NNF21OC0069598 to S.F.P., R.M., and A.S.; NNF19OC0058262 to A.S. and S.F.P.; and NNF20OC0059951 to A.S.), the Carlsberg Foundation (CF20-0491 to S.F.P. and CF19-0505 to A.S.), and The Danish Cancer Foundation (R325-A18868 to A.S. and S.F.P.).

DECLARATION OF INTERESTS

S.F.P. is a cofounder of SOLID Therapeutics.

REFERENCES

1. Mak, I.W., Evaniew, N., and Ghert, M. (2014). Lost in translation: animal models and clinical trials in cancer treatment. Am. J. Transl. Res. *6*, 114–118.
2. Kerk, S.A., Papagiannakopoulos, T., Shah, Y.M., and Lyssiotis, C.A. (2021). Metabolic networks in mutant KRAS-driven tumours: tissue specificities and the microenvironment. Nat. Rev. Cancer *21*, 510–525.
3. Mlecnik, B., Bindea, G., Kirilovsky, A., Angell, H.K., Obenauf, A.C., Tosolini, M., Church, S.E., Maby, P., Vasaturo, A., Angelova, M., et al. (2016). The tumor microenvironment and Immunoscore are critical determinants of dissemination to distant metastasis. Sci. Transl. Med. *8*, 327ra26.
4. Halbrook, C.J., Pontious, C., Kovalenko, I., Lapienyte, L., Dreyer, S., Lee, H.-J., Thurston, G., Zhang, Y., Lazarus, J., Sajjakulnukit, P., et al. (2019). Macrophage-Released Pyrimidines Inhibit Gemcitabine Therapy in Pancreatic Cancer. Cell Metab. *29*, 1390–1399.e6.
5. Wilson, W.R., and Hay, M.P. (2011). Targeting hypoxia in cancer therapy. Nat. Rev. Cancer *11*, 393–410.
6. Boedtkjer, E., and Pedersen, S.F. (2020). The Acidic Tumor Microenvironment as a Driver of Cancer. Annu. Rev. Physiol. *82*, 103–126.
7. Swietach, P., Boedtkjer, E., and Pedersen, S.F. (2023). How protons pave the way to aggressive cancers. Nat. Rev. Cancer *23*, 825–841.
8. Brown, E., Brunker, J., and Bohndiek, S.E. (2019). Photoacoustic imaging as a tool to probe the tumour microenvironment. Dis. Model. Mech *12*, dmm039636. https://doi.org/10.1242/dmm.039636.
9. Kemp Bohan, P.M., Chick, R.C., Hickerson, A.T., Messersmith, L.M., Williams, G.M., Cindass, J.L., Lombardo, J., Collins, R., Brady, R.O., Hale, D.F., et al. (2021). Correlation of tumor microenvironment from biopsy and resection specimens in untreated colorectal cancer patients: a surprising lack of agreement. Cancer Immunol. Immunother. *70*, 1465–1474.
10. Gastman, B., Agarwal, P.K., Berger, A., Boland, G., Broderick, S., Butterfield, L.H., Byrd, D., Fecci, P.E., Ferris, R.L., Fong, Y., et al. (2020). Defining best practices for tissue procurement in immuno-oncology clinical trials: consensus statement from the Society for Immunotherapy of Cancer Surgery Committee. J. Immunother. Cancer *8*, e001583. https://doi.org/10.1136/jitc-2020-001583.
11. Bott, M.J., Yang, S.C., Park, B.J., Adusumilli, P.S., Rusch, V.W., Isbell, J.M., Downey, R.J., Brahmer, J.R., Battafarano, R., Bush, E., et al. (2019). Initial results of pulmonary resection after neoadjuvant nivolumab in patients with resectable non-small cell lung cancer. J. Thorac. Cardiovasc. Surg. *158*, 269–276.
12. Ravensbergen, C.J., Kuruc, M., Polack, M., Crobach, S., Putter, H., Gelderblom, H., Roy, D., Tollenaar, R.A.E.M., and Mesker, W.E. (2021). The Stroma Liquid Biopsy Panel Contains a Stromal-Epithelial Gene Signature Ratio That Is Associated with the Histologic Tumor-Stroma Ratio and Predicts Survival in Colon Cancer. Cancers *14*, 163. https://doi.org/10.3390/cancers14010163.
13. Bareche, Y., Buisseret, L., Gruosso, T., Girard, E., Venet, D., Dupont, F., Desmedt, C., Larsimont, D., Park, M., Rothé, F., et al. (2020). Unraveling Triple-Negative Breast Cancer Tumor Microenvironment Heterogeneity: Towards an Optimized Treatment Approach. J. Natl. Cancer Inst. *112*, 708–719.
14. Elingaard-Larsen, L.O., Rolver, M.G., Sørensen, E.E., and Pedersen, S.F. (2020). How Reciprocal Interactions Between the Tumor Microenvironment and Ion Transport Proteins Drive Cancer Progression. Rev. Physiol. Biochem. Pharmacol. *182*, 1–38. https://doi.org/10.1007/112_2020_23.
15. Joyce, J.A., and Pollard, J.W. (2009). Microenvironmental regulation of metastasis. Nat. Rev. Cancer *9*, 239–252.
16. Kalluri, R. (2016). The biology and function of fibroblasts in cancer. Nat. Rev. Cancer *16*, 582–598.
17. Ridge, S.M., Sullivan, F.J., and Glynn, S.A. (2017). Mesenchymal stem cells: key players in cancer progression. Mol. Cancer *16*, 31.
18. Cox, T.R. (2021). The matrix in cancer. Nat. Rev. Cancer *21*, 217–238.
19. Liu, J.Y., and Wellen, K.E. (2020). Advances into understanding metabolites as signaling molecules in cancer progression. Curr. Opin. Cell Biol. *63*, 144–153.
20. Vogel, F.C.E., Chaves-Filho, A.B., and Schulze, A. (2024). Lipids as mediators of cancer progression and metastasis. Nat. Cancer *5*, 16–29.
21. Dranoff, G. (2004). Cytokines in cancer pathogenesis and cancer therapy. Nat. Rev. Cancer *4*, 11–22.
22. Zhang, L., and Yu, D. (2019). Exosomes in cancer development, metastasis, and immunity. Biochim. Biophys. Acta. Rev. Cancer *1871*, 455–468.
23. Curtis, C., Shah, S.P., Chin, S.-F., Turashvili, G., Rueda, O.M., Dunning, M.J., Speed, D., Lynch, A.G., Samarajiwa, S., Yuan, Y., et al. (2012). The genomic and transcriptomic architecture of 2,000 breast tumours reveals novel subgroups. Nature *486*, 346–352.
24. Ge, R., Wang, Z., and Cheng, L. (2022). Tumor microenvironment heterogeneity an important mediator of prostate cancer progression and therapeutic resistance. npj Precis. Oncol. *6*, 31.
25. Mi, H., Sivagnanam, S., Betts, C.B., Liudahl, S.M., Jaffee, E.M., Coussens, L.M., and Popel, A.S. (2022). Quantitative Spatial Profiling of Immune Populations in Pancreatic Ductal Adenocarcinoma Reveals Tumor Microenvironment Heterogeneity and Prognostic Biomarkers. Cancer Res. *82*, 4359–4372.
26. Rohani, N., Hao, L., Alexis, M.S., Joughin, B.A., Krismer, K., Moufarrej, M.N., Soltis, A.R., Lauffenburger, D.A., Yaffe, M.B., Burge, C.B., et al. (2019). Acidification of Tumor at Stromal Boundaries Drives Transcriptome Alterations Associated with Aggressive Phenotypes. Cancer Res. *79*, 1952–1966.
27. Li, F., and Simon, M.C. (2020). Cancer Cells Don't Live Alone: Metabolic Communication within Tumor Microenvironments. Dev. Cell *54*, 183–195.
28. Hjelmeland, A.B., Wu, Q., Heddleston, J.M., Choudhary, G.S., MacSwords, J., Lathia, J.D., McLendon, R., Lindner, D., Sloan, A., and Rich, J.N. (2011). Acidic stress promotes a glioma stem cell phenotype. Cell Death Differ. *18*, 829–840.
29. Huber, V., Camisaschi, C., Berzi, A., Ferro, S., Lugini, L., Triulzi, T., Tuccitto, A., Tagliabue, E., Castelli, C., and Rivoltini, L. (2017). Cancer acidity: An ultimate frontier of tumor immune escape and a novel target of immunomodulation. Semin. Cancer Biol. *43*, 74–89.
30. Lopes-Coelho, F., Martins, F., Pereira, S.A., and Serpa, J. (2021). Anti-Angiogenic Therapy: Current Challenges and Future Perspectives. Int. J. Mol. Sci. *22*, 3765. https://doi.org/10.3390/ijms22073765.
31. Provenzano, P.P., Cuevas, C., Chang, A.E., Goel, V.K., Von Hoff, D.D., and Hingorani, S.R. (2012). Enzymatic targeting of the stroma ablates physical barriers to treatment of pancreatic ductal adenocarcinoma. Cancer Cell *21*, 418–429.
32. Long, K.B., Gladney, W.L., Tooker, G.M., Graham, K., Fraietta, J.A., and Beatty, G.L. (2016). IFNγ and CCL2 Cooperate to Redirect Tumor-Infiltrating Monocytes to Degrade Fibrosis and Enhance Chemotherapy Efficacy in Pancreatic Carcinoma. Cancer Discov. *6*, 400–413.
33. Rhim, A.D., Oberstein, P.E., Thomas, D.H., Mirek, E.T., Palermo, C.F., Sastra, S.A., Dekleva, E.N., Saunders, T., Becerra, C.P., Tattersall, I.W., et al. (2014). Stromal elements act to restrain, rather than support, pancreatic ductal adenocarcinoma. Cancer Cell *25*, 735–747.
34. Mendes, N., Dias Carvalho, P., Martins, F., Mendonça, S., Malheiro, A.R., Ribeiro, A., Carvalho, J., and Velho, S. (2020). Animal Models to Study Cancer and Its Microenvironment. Adv. Exp. Med. Biol. *1219*, 389–401.

35. Jung, J., Seol, H.S., and Chang, S. (2018). The Generation and Application of Patient-Derived Xenograft Model for Cancer Research. Cancer Res. Treat. *50*, 1–10.

36. Teicher, B.A. (2006). Tumor models for efficacy determination. Mol. Cancer Ther. *5*, 2435–2443.

37. Sharpless, N.E., and Depinho, R.A. (2006). The mighty mouse: genetically engineered mouse models in cancer drug development. Nat. Rev. Drug Discov. *5*, 741–754.

38. Day, C.-P., Merlino, G., and Van Dyke, T. (2015). Preclinical mouse cancer models: a maze of opportunities and challenges. Cell *163*, 39–53.

39. Fiebig, H.H., Schuchhardt, C., Henss, H., Fiedler, L., and Löhr, G.W. (1984). Comparison of tumor response in nude mice and in the patients. Behring Inst. Mitt., 343–352.

40. Yada, E., Wada, S., Yoshida, S., and Sasada, T. (2018). Use of patient-derived xenograft mouse models in cancer research and treatment. Future Sci. OA *4*, FSO271.

41. Hidalgo, M., Bruckheimer, E., Rajeshkumar, N.V., Garrido-Laguna, I., De Oliveira, E., Rubio-Viqueira, B., Strawn, S., Wick, M.J., Martell, J., and Sidransky, D. (2011). A pilot clinical study of treatment guided by personalized tumorgrafts in patients with advanced cancer. Mol. Cancer Ther. *10*, 1311–1316.

42. Siolas, D., and Hannon, G.J. (2013). Patient-derived tumor xenografts: transforming clinical samples into mouse models. Cancer Res. *73*, 5315–5319.

43. Castillo-Ecija, H., Pascual-Pasto, G., Perez-Jaume, S., Resa-Pares, C., Vila-Ubach, M., Monterrubio, C., Jimenez-Cabaco, A., Baulenas-Farres, M., Muñoz-Aznar, O., Salvador, N., et al. (2021). Prognostic value of patient-derived xenograft engraftment in pediatric sarcomas. Hip Int. *7*, 338–349.

44. Cassidy, J.W., Caldas, C., and Bruna, A. (2015). Maintaining Tumor Heterogeneity in Patient-Derived Tumor Xenografts. Cancer Res. *75*, 2963–2968.

45. Martinov, T., McKenna, K.M., Tan, W.H., Collins, E.J., Kehret, A.R., Linton, J.D., Olsen, T.M., Shobaki, N., and Rongvaux, A. (2021). Building the Next Generation of Humanized Hemato-Lymphoid System Mice. Front. Immunol. *12*, 643852.

46. Zhao, Y., Shuen, T.W.H., Toh, T.B., Chan, X.Y., Liu, M., Tan, S.Y., Fan, Y., Yang, H., Lyer, S.G., Bonney, G.K., et al. (2018). Development of a new patient-derived xenograft humanised mouse model to study human-specific tumour microenvironment and immunotherapy. Gut *67*, 1845–1854.

47. Verma, B., and Wesa, A. (2020). Establishment of Humanized Mice from Peripheral Blood Mononuclear Cells or Cord Blood CD34+ Hematopoietic Stem Cells for Immune-Oncology Studies Evaluating New Therapeutic Agents. Curr. Protoc. Pharmacol. *89*, e77.

48. Cogels, M.M., Rouas, R., Ghanem, G.E., Martinive, P., Awada, A., Van Gestel, D., and Krayem, M. (2021). Humanized Mice as a Valuable Pre-Clinical Model for Cancer Immunotherapy Research. Front. Oncol. *11*, 784947.

49. Lan, P., Tonomura, N., Shimizu, A., Wang, S., and Yang, Y.-G. (2006). Reconstitution of a functional human immune system in immunodeficient mice through combined human fetal thymus/liver and CD34+ cell transplantation. Blood *108*, 487–492.

50. Melkus, M.W., Estes, J.D., Padgett-Thomas, A., Gatlin, J., Denton, P.W., Othieno, F.A., Wege, A.K., Haase, A.T., and Garcia, J.V. (2006). Humanized mice mount specific adaptive and innate immune responses to EBV and TSST-1. Nat. Med. *12*, 1316–1322.

51. Lechner, M.G., Karimi, S.S., Barry-Holson, K., Angell, T.E., Murphy, K.A., Church, C.H., Ohlfest, J.R., Hu, P., and Epstein, A.L. (2013). Immunogenicity of murine solid tumor models as a defining feature of in vivo behavior and response to immunotherapy. J. Immunother. *36*, 477–489.

52. Yu, J.W., Bhattacharya, S., Yanamandra, N., Kilian, D., Shi, H., Yadavilli, S., Katlinskaya, Y., Kaczynski, H., Conner, M., Benson, W., et al. (2018). Tumor-immune profiling of murine syngeneic tumor models as a framework to guide mechanistic studies and predict therapy response in distinct tumor microenvironments. PLoS One *13*, e0206223.

53. Liu, Y., Yin, T., Feng, Y., Cona, M.M., Huang, G., Liu, J., Song, S., Jiang, Y., Xia, Q., Swinnen, J.V., et al. (2015). Mammalian models of chemically induced primary malignancies exploitable for imaging-based preclinical theragnostic research. Quant. Imag. Med. Surg. *5*, 708–729.

54. Lee, S., Axelsen, T.V., Andersen, A.P., Vahl, P., Pedersen, S.F., and Boedtkjer, E. (2016). Disrupting Na^+, HCO_3^--cotransporter NBCn1 (Slc4a7) delays murine breast cancer development. Oncogene *35*, 2112–2122.

55. Kersten, K., de Visser, K.E., van Miltenburg, M.H., and Jonkers, J. (2017). Genetically engineered mouse models in oncology research and cancer medicine. EMBO Mol. Med. *9*, 137–153.

56. Heyer, J., Kwong, L.N., Lowe, S.W., and Chin, L. (2010). Non-germline genetically engineered mouse models for translational cancer research. Nat. Rev. Cancer *10*, 470–480.

57. García-Cañaveras, J.C., Chen, L., and Rabinowitz, J.D. (2019). The Tumor Metabolic Microenvironment: Lessons from Lactate. Cancer Res. *79*, 3155–3162.

58. Barker, H.E., Cox, T.R., and Erler, J.T. (2012). The rationale for targeting the LOX family in cancer. Nat. Rev. Cancer *12*, 540–552.

59. Ibrahim-Hashim, A., Abrahams, D., Enriquez-Navas, P.M., Luddy, K., Gatenby, R.A., and Gillies, R.J. (2017). Tris-base buffer: a promising new inhibitor for cancer progression and metastasis. Cancer Med. *6*, 1720–1729.

60. Semenza, G.L. (2023). Targeting intratumoral hypoxia to enhance anti-tumor immunity. Semin. Cancer Biol. *96*, 5–10.

61. Sarode, G.S., Sarode, S.C., Gadbail, A.R., Gondivkar, S., Sharma, N.K., and Patil, S. (2019). Lysyl oxidase in oral cancer: Friend or foe? Med. Hypotheses *130*, 109283.

62. Voss, N.C.S., Dreyer, T., Henningsen, M.B., Vahl, P., Honoré, B., and Boedtkjer, E. (2020). Targeting the Acidic Tumor Microenvironment: Unexpected Pro-Neoplastic Effects of Oral NaHCO Therapy in Murine Breast Tissue. Cancers *12*, 891. https://doi.org/10.3390/cancers12040891.

63. Howe, K., Clark, M.D., Torroja, C.F., Torrance, J., Berthelot, C., Muffato, M., Collins, J.E., Humphray, S., McLaren, K., Matthews, L., et al. (2013). The zebrafish reference genome sequence and its relationship to the human genome. Nature *496*, 498–503.

64. Fior, R., Póvoa, V., Mendes, R.V., Carvalho, T., Gomes, A., Figueiredo, N., and Ferreira, M.G. (2017). Single-cell functional and chemosensitive profiling of combinatorial colorectal therapy in zebrafish xenografts. Proc. Natl. Acad. Sci. USA *114*, E8234–E8243.

65. White, R.M., Sessa, A., Burke, C., Bowman, T., LeBlanc, J., Ceol, C., Bourque, C., Dovey, M., Goessling, W., Burns, C.E., and Zon, L.I. (2008). Transparent adult zebrafish as a tool for in vivo transplantation analysis. Cell Stem Cell *2*, 183–189.

66. Mione, M.C., and Trede, N.S. (2010). The zebrafish as a model for cancer. Dis. Model. Mech. *3*, 517–523.

67. Osmani, N., and Goetz, J.G. (2019). Multiscale Imaging of Metastasis in Zebrafish. Trends Cancer *5*, 766–778.

68. Shive, H.R. (2013). Zebrafish models for human cancer. Vet. Pathol. *50*, 468–482.

69. Weiss, J.M., Lumaquin-Yin, D., Montal, E., Suresh, S., Leonhardt, C.S., and White, R.M. (2022). Shifting the focus of zebrafish toward a model of the tumor microenvironment. Elife *11*, e69703. https://doi.org/10.7554/eLife.69703.

70. Kirchberger, S., Sturtzel, C., Pascoal, S., and Distel, M. (2017). ?Recent Progress in Modeling Cancer in Zebrafish. Front. Oncol. *7*, 186.

71. Bilder, D., Ong, K., Hsi, T.-C., Adiga, K., and Kim, J. (2021). Tumour-host interactions through the lens of Drosophila. Nat. Rev. Cancer *21*, 687–700.

72. Chatterjee, D., and Deng, W.-M. (2019). Drosophila Model in Cancer: An Introduction. Adv. Exp. Med. Biol. *1167*, 1–14.

73. Katheder, N.S., Khezri, R., O'Farrell, F., Schultz, S.W., Jain, A., Rahman, M.M., Schink, K.O., Theodossiou, T.A., Johansen, T., Juhász, G., et al. (2017). Microenvironmental autophagy promotes tumour growth. Nature *541*, 417–420.

74. Zhao, H., Shi, L., Kong, R., Li, Z., Liu, F., Zhao, H., and Li, Z. (2021). Autophagy induction in tumor surrounding cells promotes tumor growth in adult Drosophila intestines. Dev. Biol. *476*, 294–307.

75. Pastor-Pareja, J.C., Wu, M., and Xu, T. (2008). An innate immune response of blood cells to tumors and tissue damage in Drosophila. Dis. Model. Mech. *1*, 144–154. discussion 153.

76. Stuelten, C.H., Parent, C.A., and Montell, D.J. (2018). Cell motility in cancer invasion and metastasis: insights from simple model organisms. Nat. Rev. Cancer *18*, 296–312.

77. Czaplinska, D., Elingaard-Larsen, L.O., Rolver, M.G., Severin, M., and Pedersen, S.F. (2019). 3D multicellular models to study the regulation and roles of acid-base transporters in breast cancer. Biochem. Soc. Trans. *47*, 1689–1700.

78. Hirschhaeuser, F., Menne, H., Dittfeld, C., West, J., Mueller-Klieser, W., and Kunz-Schughart, L.A. (2010). Multicellular tumor spheroids: an underestimated tool is catching up again. J. Biotechnol. *148*, 3–15.

79. Han, K., Pierce, S.E., Li, A., Spees, K., Anderson, G.R., Seoane, J.A., Lo, Y.-H., Dubreuil, M., Olivas, M., Kamber, R.A., et al. (2020). CRISPR screens in cancer spheroids identify 3D growth-specific vulnerabilities. Nature *580*, 136–141.

80. Takahashi, N., Cho, P., Selfors, L.M., Kuiken, H.J., Kaul, R., Fujiwara, T., Harris, I.S., Zhang, T., Gygi, S.P., and Brugge, J.S. (2020). 3D Culture Models with CRISPR Screens Reveal Hyperactive NRF2 as a Prerequisite for Spheroid Formation via Regulation of Proliferation and Ferroptosis. Mol. Cell *80*, 828–844.e6.

81. Caliari, S.R., and Burdick, J.A. (2016). A practical guide to hydrogels for cell culture. Nat. Methods *13*, 405–414.

82. Rafaeva, M., Horton, E.R., Jensen, A.R.D., Madsen, C.D., Reuten, R., Willacy, O., Brøchner, C.B., Jensen, T.H., Zornhagen, K.W., Crespo, M., et al. (2022). Modeling Metastatic Colonization in a Decellularized Organ Scaffold-Based Perfusion Bioreactor. Adv. Healthc. Mater. *11*, e2100684.

83. Sato, T., Vries, R.G., Snippert, H.J., van de Wetering, M., Barker, N., Stange, D.E., van Es, J.H., Abo, A., Kujala, P., Peters, P.J., and Clevers, H. (2009). Single Lgr5 stem cells build crypt-villus structures in vitro without a mesenchymal niche. Nature *459*, 262–265.

84. Ootani, A., Li, X., Sangiorgi, E., Ho, Q.T., Ueno, H., Toda, S., Sugihara, H., Fujimoto, K., Weissman, I.L., Capecchi, M.R., and Kuo, C.J. (2009). Sustained in vitro intestinal epithelial culture within a Wnt-dependent stem cell niche. Nat. Med. *15*, 701–706.

85. Yuki, K., Cheng, N., Nakano, M., and Kuo, C.J. (2020). Organoid Models of Tumor Immunology. Trends Immunol. *41*, 652–664.

86. Drost, J., and Clevers, H. (2018). Organoids in cancer research. Nat. Rev. Cancer *18*, 407–418.

87. Vilgelm, A.E., Bergdorf, K., Wolf, M., Bharti, V., Shattuck-Brandt, R., Blevins, A., Jones, C., Phifer, C., Lee, M., Lowe, C., et al. (2020). Fine-Needle Aspiration-Based Patient-Derived Cancer Organoids. iScience *23*, 101408.

88. (2018). Tumor Evolution and Drug Response in Patient-Derived Organoid Models of Bladder Cancer. Cell *173*, 515–528.e17.

89. Wörsdörfer, P., Dalda, N., Kern, A., Krüger, S., Wagner, N., Kwok, C.K., Henke, E., and Ergün, S. (2019). Generation of complex human organoid models including vascular networks by incorporation of mesodermal progenitor cells. Sci. Rep. *9*, 15663.

90. Yip, S., Wang, N., and Sugimura, R. (2023). Give Them Vasculature and Immune Cells: How to Fill the Gap of Organoids. Cells Tissues Organs *212*, 369–382.

91. Chakrabarti, J., Koh, V., Steele, N., Hawkins, J., Ito, Y., Merchant, J.L., Wang, J., Helmrath, M.A., Ahmad, S.A., So, J.B.Y., et al. (2021). Disruption of Her2-Induced PD-L1 Inhibits Tumor Cell Immune Evasion in Patient-Derived Gastric Cancer Organoids. Cancers *13*, 6158. https://doi.org/10.3390/cancers13246158.

92. Hubert, C.G., Rivera, M., Spangler, L.C., Wu, Q., Mack, S.C., Prager, B.C., Couce, M., McLendon, R.E., Sloan, A.E., and Rich, J.N. (2016). A Three-Dimensional Organoid Culture System Derived from Human Glioblastomas Recapitulates the Hypoxic Gradients and Cancer Stem Cell Heterogeneity of Tumors Found In Vivo. Cancer Res. *76*, 2465–2477.

93. Neal, J.T., Li, X., Zhu, J., Giangarra, V., Grzeskowiak, C.L., Ju, J., Liu, I.H., Chiou, S.-H., Salahudeen, A.A., Smith, A.R., et al. (2018). Organoid Modeling of the Tumor Immune Microenvironment. Cell *175*, 1972–1988.e16.

94. Courau, T., Bonnereau, J., Chicoteau, J., Bottois, H., Remark, R., Assante Miranda, L., Toubert, A., Blery, M., Aparicio, T., Allez, M., and Le Bourhis, L. (2019). Cocultures of human colorectal tumor spheroids with immune cells reveal the therapeutic potential of MICA/B and NKG2A targeting for cancer treatment. J. Immunother. Cancer *7*, 74.

95. Tsai, S., McOlash, L., Palen, K., Johnson, B., Duris, C., Yang, Q., Dwinell, M.B., Hunt, B., Evans, D.B., Gershan, J., and James, M.A. (2018). Development of primary human pancreatic cancer organoids, matched stromal and immune cells and 3D tumor microenvironment models. BMC Cancer *18*, 335.

96. Pine, A.R., Cirigliano, S.M., Nicholson, J.G., Hu, Y., Linkous, A., Miyaguchi, K., Edwards, L., Singhania, R., Schwartz, T.H., Ramakrishna, R., et al. (2020). Tumor Microenvironment Is Critical for the Maintenance of Cellular States Found in Primary Glioblastomas. Cancer Discov. *10*, 964–979.

97. Squires, T.M., and Quake, S.R. (2005). Microfluidics: Fluid physics at the nanoliter scale. Rev. Mod. Phys. *77*, 977. https://doi.org/10.1103/revmodphys.77.977.

98. Chang, T.C., Mikheev, A.M., Huynh, W., Monnat, R.J., Rostomily, R.C., and Folch, A. (2014). Parallel microfluidic chemosensitivity testing on individual slice cultures. Lab Chip *14*, 4540–4551. https://doi.org/10.1039/c4lc00642a.

99. Astolfi, M., Péant, B., Lateef, M.A., Rousset, N., Kendall-Dupont, J., Carmona, E., Monet, F., Saad, F., Provencher, D., Mes-Masson, A.-M., et al. (2016). Micro-dissected tumor tissues on chip: an ex vivo method for drug testing and personalized therapy. Lab Chip *16*, 312–325. https://doi.org/10.1039/c5lc01108f.

100. Horowitz, L.F., Rodriguez, A.D., Dereli-Korkut, Z., Lin, R., Castro, K., Mikheev, A., Monnat, R.J., Folch, A., and Rostomily, R.C. (2020). Multiplexed drug testing of tumor slices using a microfluidic platform. Lab Chip *20*, 1658–1675. https://doi.org/10.1101/2020.02.25.965137.

101. Follain, G., Herrmann, D., Harlepp, S., Hyenne, V., Osmani, N., Warren, S.C., Timpson, P., and Goetz, J.G. (2020). Fluids and their mechanics in tumour transit: shaping metastasis. Nat. Rev. Cancer *20*, 107–124.

102. Rizvi, I., Gurkan, U.A., Tasoglu, S., Alagic, N., Celli, J.P., Mensah, L.B., Mai, Z., Demirci, U., and Hasan, T. (2013). Flow induces epithelial-mesenchymal transition, cellular heterogeneity and biomarker modulation in 3D ovarian cancer nodules. Proc. Natl. Acad. Sci. USA *110*, E1974–E1983. https://doi.org/10.1073/pnas.1216989110.

103. Huang, Y.L., Tung, C.-K., Zheng, A., Kim, B.J., and Wu, M. (2015). Interstitial flows promote amoeboid over mesenchymal motility of breast cancer cells revealed by a three dimensional microfluidic model. Integr. Biol. *7*, 1402–1411. https://doi.org/10.1039/c5ib00115c.

104. Polacheck, W.J., German, A.E., Mammoto, A., Ingber, D.E., and Kamm, R.D. (2014). Mechanotransduction of fluid stresses governs 3D cell migration. Proc. Natl. Acad. Sci. USA *111*, 2447–2452.

105. Li, R., Serrano, J.C., Xing, H., Lee, T.A., Azizgolshani, H., Zaman, M., and Kamm, R.D. (2018). Interstitial flow promotes macrophage polarization toward an M2 phenotype. Mol. Biol. Cell *29*, 1927–1940.

106. Song, C., Gao, D., Yuan, T., Chen, Y., Liu, L., Chen, X., and Jiang, Y. (2019). Microfluidic three-dimensional biomimetic tumor model for studying breast cancer cell migration and invasion in the presence of interstitial flow. Chin. Chem. Lett. *30*, 1038–1042.

107. Lee, G.-H., Huang, S.A., Aw, W.Y., Rathod, M.L., Cho, C., Ligler, F.S., and Polacheck, W.J. (2022). Multilayer microfluidic platform for the study of luminal, transmural, and interstitial flow. Biofabrication *14*, 025007. https://doi.org/10.1088/1758-5090/ac48e5.

108. Kwak, B., Ozcelikkale, A., Shin, C.S., Park, K., and Han, B. (2014). Simulation of complex transport of nanoparticles around a tumor using tumor-microenvironment-on-chip. J Control Release *194*, 157–167. https://doi.org/10.1016/j.jconrel.2014.08.027.

109. Onal, S., Alkaisi, M.M., and Nock, V. (2021). A Flexible Microdevice for Mechanical Cell Stimulation and Compression in Microfluidic Settings. Front. Phys *9*, 654918. https://doi.org/10.3389/fphy.2021.654918.

110. Ayuso, J.M., Virumbrales-Munoz, M., McMinn, P.H., Rehman, S., Gomez, I., Karim, M.R., Trusttchel, R., Wisinski, K.B., Beebe, D.J., and Skala, M.C. (2019). Tumor-on-a-chip: a microfluidic model to study cell response to environmental gradients. Lab Chip *19*, 3461–3471. https://doi.org/10.1039/c9lc00270g.

111. Stylianopoulos, T., Munn, L.L., and Jain, R.K. (2018). Reengineering the Physical Microenvironment of Tumors to Improve Drug Delivery and Efficacy: From Mathematical Modeling to Bench to Bedside. Trends Cancer *4*, 292–319. https://doi.org/10.1016/j.trecan.2018.02.005.

112. Ariffin, A.B., Forde, P.F., Jahangeer, S., Soden, D.M., and Hinchion, J. (2014). Releasing Pressure in Tumors: What Do We Know So Far and Where Do We Go from Here? A Review. Cancer Res. *74*, 2655–2662. https://doi.org/10.1158/0008-5472.can-13-3696.

113. Stylianopoulos, T., Martin, J.D., Snuderl, M., Mpekris, F., Jain, S.R., and Jain, R.K. (2013). Coevolution of solid stress and interstitial fluid pressure in tumors during progression: implications for vascular collapse. Cancer Res. *73*, 3833–3841.

114. Nia, H.T., Munn, L.L., and Jain, R.K. (2020). Physical traits of cancer. Science *370*, eaaz0868. https://doi.org/10.1126/science.aaz0868.

115. Buchanan, C.F., Verbridge, S.S., Vlachos, P.P., and Rylander, M.N. (2014). Flow shear stress regulates endothelial barrier function and expression of angiogenic factors in a 3D microfluidic tumor vascular model. Cell Adh. Migr. *8*, 517–524. https://doi.org/10.4161/19336918.2014.970001.

116. Voutouri, C., and Stylianopoulos, T. (2014). Evolution of osmotic pressure in solid tumors. J. Biomech. *47*, 3441–3447. https://doi.org/10.1016/j.jbiomech.2014.09.019.

117. Hui, T.H., Cho, W.C., Fong, H.W., Yu, M., Kwan, K.W., Ngan, K.C., Wong, K.H., Tan, Y., Yao, S., Jiang, H., et al. (2019). An electro-osmotic microfluidic system to characterize cancer cell migration under confinement. J R Soc. Interface *16*, 20190062. https://doi.org/10.1098/rsif.2019.0062.

118. Douville, N.J., Zamankhan, P., Tung, Y.-C., Li, R., Vaughan, B.L., Tai, C.-F., White, J., Christensen, P.J., Grotberg, J.B., and Takayama, S. (2011). Combination of fluid and solid mechanical stresses contribute to cell death and detachment in a microfluidic alveolar model. Lab Chip *11*, 609–619. https://doi.org/10.1039/c0lc00251h.

119. Wang, S.-J., Saadi, W., Lin, F., Minh-Canh Nguyen, C., and Li Jeon, N. (2004). Differential effects of EGF gradient profiles on MDA-MB-231 breast cancer cell chemotaxis. Exp. Cell Res. *300*, 180–189. https://doi.org/10.1016/j.yexcr.2004.06.030.

120. Koens, R., Tabata, Y., Serrano, J.C., Aratake, S., Yoshino, D., Kamm, R.D., and Funamoto, K. (2020). Microfluidic platform for three-dimensional cell culture under spatiotemporal heterogeneity of oxygen tension. APL Bioeng. *4*, 016106. https://doi.org/10.1063/1.5127069.

121. Grist, S.M., Nasseri, S.S., Laplatine, L., Schmok, J.C., Yao, D., Hua, J., Chrostowski, L., and Cheung, K.C. (2019). Long-term monitoring in a microfluidic system to study tumour spheroid response to chronic and cycling hypoxia. Sci. Rep. *9*, 17782. https://doi.org/10.1038/s41598-019-54001-8.

122. Bersini, S., Jeon, J.S., Dubini, G., Arrigoni, C., Chung, S., Charest, J.L., Moretti, M., and Kamm, R.D. (2014). A microfluidic 3D in vitro model for specificity of breast cancer metastasis to bone. Biomaterials *35*, 2454–2461. https://doi.org/10.1016/j.biomaterials.2013.11.050.

123. Cavnar, S.P., Ray, P., Moudgil, P., Chang, S.L., Luker, K.E., Linderman, J.J., Takayama, S., and Luker, G.D. (2014). Microfluidic source-sink model reveals effects of biophysically distinct CXCL12 isoforms in breast cancer chemotaxis. Integr. Biol. *6*, 564–576.

124. Lou, X., Kim, G., Yoon, H.K., Lee, Y.-E.K., Kopelman, R., and Yoon, E. (2014). A high-throughput photodynamic therapy screening platform with on-chip control of multiple microenvironmental factors. Lab Chip *14*, 892–901.

125. Kim, S., Lee, H., Chung, M., and Jeon, N.L. (2013). Engineering of functional, perfusable 3D microvascular networks on a chip. Lab Chip *13*, 1489. https://doi.org/10.1039/c3lc41320a.

126. Miller, C.P., Tsuchida, C., Zheng, Y., Himmelfarb, J., and Akilesh, S. (2018). A 3D Human Renal Cell Carcinoma-on-a-Chip for the Study of Tumor Angiogenesis. Neoplasia *20*, 610–620.

127. Hassell, B.A., Goyal, G., Lee, E., Sontheimer-Phelps, A., Levy, O., Chen, C.S., and Ingber, D.E. (2017). Human Organ Chip Models Recapitulate Orthotopic Lung Cancer Growth, Therapeutic Responses, and Tumor Dormancy In Vitro. Cell Rep. *21*, 508–516.

128. Lee, J.-H., Kim, S.-K., Khawar, I.A., Jeong, S.-Y., Chung, S., and Kuh, H.-J. (2018). Microfluidic co-culture of pancreatic tumor spheroids with stellate cells as a novel 3D model for investigation of stroma-mediated cell motility and drug resistance. J. Exp. Clin. Cancer Res. *37*, 4.

129. Fang, G., Lu, H., Rodriguez de la Fuente, L., Law, A.M.K., Lin, G., Jin, D., and Gallego-Ortega, D. (2021). Mammary Tumor Organoid Culture in Non-Adhesive Alginate for Luminal Mechanics and High-Throughput Drug Screening. Adv. Sci. *8*, e2102418.

130. Sontheimer-Phelps, A., Hassell, B.A., and Ingber, D.E. (2019). Modelling cancer in microfluidic human organs-on-chips. Nat. Rev. Cancer *19*, 65–81.

131. Zhou, Z., Cong, L., and Cong, X. (2021). Patient-Derived Organoids in Precision Medicine: Drug Screening, Organoid-on-a-Chip and Living Organoid Biobank. Front. Oncol. *11*, 762184.

132. Whitesides, G.M., Ostuni, E., Takayama, S., Jiang, X., and Ingber, D.E. (2001). Soft lithography in biology and biochemistry. Annu. Rev. Biomed. Eng. *3*, 335–373.

133. Takebe, T., Zhang, B., and Radisic, M. (2017). Synergistic Engineering: Organoids Meet Organs-on-a-Chip. Cell Stem Cell *21*, 297–300.

134. Dornhof, J., Kieninger, J., Muralidharan, H., Maurer, J., Urban, G.A., and Weltin, A. (2022). Microfluidic organ-on-chip system for multi-analyte monitoring of metabolites in 3D cell cultures. Lab Chip *22*, 225–239.

135. Haque, M.R., Wessel, C.R., Leary, D.D., Wang, C., Bhushan, A., and Bishehsari, F. (2022). Patient-derived pancreatic cancer-on-a-chip recapitulates the tumor microenvironment. Microsyst. Nanoeng. *8*, 36.

136. Auxillos, J., Crouigneau, R., Li, Y.-F., Dai, Y., Stigliani, A., Tavernaro, I., Resch-Genger, U., Sandelin, A., Marie, R., and Pedersen, S.F. (2024). Spatially resolved analysis of microenvironmental gradient impact on cancer cell phenotypes. Sci. Adv. *10*, eadn3448.

137. Fang, G., Lu, H., Al-Nakashli, R., Chapman, R., Zhang, Y., Ju, L.A., Lin, G., Stenzel, M.H., and Jin, D. (2021). Enabling peristalsis of human colon tumor organoids on microfluidic chips. Biofabrication *14*. https://doi.org/10.1088/1758-5090/ac2ef9.

138. Ohno, Y., Nishio, M., Koyama, H., Miura, S., Yoshikawa, T., Matsumoto, S., and Sugimura, K. (2014). Dynamic contrast-enhanced CT and MRI for pulmonary nodule assessment. AJR Am. J. Roentgenol. *202*, 515–529.

139. Hallac, R.R., Zhou, H., Pidikiti, R., Song, K., Stojadinovic, S., Zhao, D., Solberg, T., Peschke, P., and Mason, R.P. (2014). Correlations of

noninvasive BOLD and TOLD MRI with pO2 and relevance to tumor radiation response. Magn. Reson. Med. *71*, 1863–1873.

140. Howe, F.A., Robinson, S.P., McIntyre, D.J., Stubbs, M., and Griffiths, J.R. (2001). Issues in flow and oxygenation dependent contrast (FLOOD) imaging of tumours. NMR Biomed. *14*, 497–506.
141. Muzard, J., Sarda-Mantel, L., Loyau, S., Meulemans, A., Louedec, L., Bantsimba-Malanda, C., Hervatin, F., Marchal-Somme, J., Michel, J.B., Le Guludec, D., et al. (2009). Non-invasive molecular imaging of fibrosis using a collagen-targeted peptidomimetic of the platelet collagen receptor glycoprotein VI. PLoS One *4*, e5585.
142. Akkaya, H.E., Erden, A., Kuru Öz, D., Ünal, S., and Erden, İ. (2018). Magnetic resonance elastography: basic principles, technique, and clinical applications in the liver. Diagn. Interv. Radiol. *24*, 328–335.
143. Lilburn, D.M.L., and Groves, A.M. (2021). The role of PET in imaging of the tumour microenvironment and response to immunotherapy. Clin. Radiol. *76*, 784.e1–784.e15.
144. Wang, L.V., and Yao, J. (2016). A practical guide to photoacoustic tomography in the life sciences. Nat. Methods *13*, 627–638.
145. Pan, X., Gao, A., and Lin, Z. (2022). Fluorescence imaging of tumor immune contexture in immune checkpoint blockade therapy. Int. Immunopharmacol. *106*, 108617.
146. Bousso, P. (2022). Diving into the mechanism of action of tumor immunotherapies with intravital imaging. Immunol. Rev. *306*, 218–223.
147. Cahalan, M.D., Parker, I., Wei, S.H., and Miller, M.J. (2002). Two-photon tissue imaging: seeing the immune system in a fresh light. Nat. Rev. Immunol. *2*, 872–880.
148. Wu, C., Mao, Y., Wang, X., Li, P., and Tang, B. (2022). Deep-Tissue Fluorescence Imaging Study of Reactive Oxygen Species in a Tumor Microenvironment. Anal. Chem. *94*, 165–176.
149. Gerdes, M.J., Sevinsky, C.J., Sood, A., Adak, S., Bello, M.O., Bordwell, A., Can, A., Corwin, A., Dinn, S., Filkins, R.J., et al. (2013). Highly multiplexed single-cell analysis of formalin-fixed, paraffin-embedded cancer tissue. Proc. Natl. Acad. Sci. USA *110*, 11982–11987.
150. Angelo, M., Bendall, S.C., Finck, R., Hale, M.B., Hitzman, C., Borowsky, A.D., Levenson, R.M., Lowe, J.B., Liu, S.D., Zhao, S., et al. (2014). Multiplexed ion beam imaging of human breast tumors. Nat. Med. *20*, 436–442.
151. Goltsev, Y., Samusik, N., Kennedy-Darling, J., Bhate, S., Hale, M., Vazquez, G., Black, S., and Nolan, G.P. (2018). Deep Profiling of Mouse Splenic Architecture with CODEX Multiplexed Imaging. Cell *174*, 968–981.e15.
152. Elhanani, O., Ben-Uri, R., and Keren, L. (2023). Spatial profiling technologies illuminate the tumor microenvironment. Cancer Cell *41*, 404–420.
153. Wang, F., Flanagan, J., Su, N., Wang, L.-C., Bui, S., Nielson, A., Wu, X., Vo, H.-T., Ma, X.-J., and Luo, Y. (2012). RNAscope: a novel in situ RNA analysis platform for formalin-fixed, paraffin-embedded tissues. J. Mol. Diagn. *14*, 22–29.
154. Jeong, H.Y., Ham, I.-H., Lee, S.H., Ryu, D., Son, S.-Y., Han, S.-U., Kim, T.-M., and Hur, H. (2021). Spatially Distinct Reprogramming of the Tumor Microenvironment Based On Tumor Invasion in Diffuse-Type Gastric Cancers. Clin. Cancer Res. *27*, 6529–6542.
155. Chen, K.H., Boettiger, A.N., Moffitt, J.R., Wang, S., and Zhuang, X. (2015). RNA imaging. Spatially resolved, highly multiplexed RNA profiling in single cells. Science *348*, aaa6090.
156. Hara, T., Chanoch-Myers, R., Mathewson, N.D., Myskiw, C., Atta, L., Bussema, L., Eichhorn, S.W., Greenwald, A.C., Kinker, G.S., Rodman, C., et al. (2021). Interactions between cancer cells and immune cells drive transitions to mesenchymal-like states in glioblastoma. Cancer Cell *39*, 779–792.e11.
157. Planque, M., Igelmann, S., Ferreira Campos, A.M., and Fendt, S.-M. (2023). Spatial metabolomics principles and application to cancer research. Curr. Opin. Chem. Biol. *76*, 102362.
158. Walsh, L.A., and Quail, D.F. (2023). Decoding the tumor microenvironment with spatial technologies. Nat. Immunol. *24*, 1982–1993.
159. Hoadley, K.A., Yau, C., Wolf, D.M., Cherniack, A.D., Tamborero, D., Ng, S., Leiserson, M.D.M., Niu, B., McLellan, M.D., Uzunangelov, V., et al. (2014). Multiplatform analysis of 12 cancer types reveals molecular classification within and across tissues of origin. Cell *158*, 929–944.
160. Rheinbay, E., Nielsen, M.M., Abascal, F., Wala, J.A., Shapira, O., Tiao, G., Hornshøj, H., Hess, J.M., Juul, R.I., Lin, Z., et al. (2020). Analyses of non-coding somatic drivers in 2,658 cancer whole genomes. Nature *578*, 102–111.
161. Andor, N., Graham, T.A., Jansen, M., Xia, L.C., Aktipis, C.A., Petritsch, C., Ji, H.P., and Maley, C.C. (2016). Pan-cancer analysis of the extent and consequences of intratumor heterogeneity. Nat. Med. *22*, 105–113.
162. Sobral, D., Martins, M., Kaplan, S., Golkaram, M., Salmans, M., Khan, N., Vijayaraghavan, R., Casimiro, S., Fernandes, A., Borralho, P., et al. (2022). Genetic and microenvironmental intra-tumor heterogeneity impacts colorectal cancer evolution and metastatic development. Commun. Biol. *5*, 937.
163. Evrony, G.D., Hinch, A.G., and Luo, C. (2021). Applications of Single-Cell DNA Sequencing. Annu. Rev. Genomics Hum. Genet. *22*, 171–197.
164. Gawad, C., Koh, W., and Quake, S.R. (2016). Single-cell genome sequencing: current state of the science. Nat. Rev. Genet. *17*, 175–188.
165. Zhao, T., Chiang, Z.D., Morriss, J.W., LaFave, L.M., Murray, E.M., Del Priore, I., Meli, K., Lareau, C.A., Nadaf, N.M., Li, J., et al. (2022). Spatial genomics enables multi-modal study of clonal heterogeneity in tissues. Nature *601*, 85–91.
166. Ozsolak, F., and Milos, P.M. (2011). RNA sequencing: advances, challenges and opportunities. Nat. Rev. Genet. *12*, 87–98.
167. Conesa, A., Madrigal, P., Tarazona, S., Gomez-Cabrero, D., Cervera, A., McPherson, A., Szcześniak, M.W., Gaffney, D.J., Elo, L.L., Zhang, X., and Mortazavi, A. (2016). A survey of best practices for RNA-seq data analysis. Genome Biol. *17*, 13–19.
168. Amarasinghe, S.L., Su, S., Dong, X., Zappia, L., Ritchie, M.E., and Gouil, Q. (2020). Opportunities and challenges in long-read sequencing data analysis. Genome Biol. *21*, 30.
169. Yao, J., Czaplinska, D., Ialchina, R., Schnipper, J., Liu, B., Sandelin, A., and Pedersen, S.F. (2020). Cancer Cell Acid Adaptation Gene Expression Response Is Correlated to Tumor-Specific Tissue Expression Profiles and Patient Survival. Cancers *12*, 2183. https://doi.org/10.3390/cancers12082183.
170. Haque, A., Engel, J., Teichmann, S.A., and Lönnberg, T. (2017). A practical guide to single-cell RNA-sequencing for biomedical research and clinical applications. Genome Med. *9*, 75.
171. Stuart, T., and Satija, R. (2019). Integrative single-cell analysis. Nat. Rev. Genet. *20*, 257–272.
172. Tran, H.T.N., Ang, K.S., Chevrier, M., Zhang, X., Lee, N.Y.S., Goh, M., and Chen, J. (2020). A benchmark of batch-effect correction methods for single-cell RNA sequencing data. Genome Biol. *21*, 12.
173. Luecken, M.D., and Theis, F.J. (2019). Current best practices in single-cell RNA-seq analysis: a tutorial. Mol. Syst. Biol. *15*, e8746.
174. Wagner, D.E., and Klein, A.M. (2020). Lineage tracing meets single-cell omics: opportunities and challenges. Nat. Rev. Genet. *21*, 410–427.
175. McCarthy, D.J., Rostom, R., Huang, Y., Kunz, D.J., Danecek, P., Bonder, M.J., Hagai, T., Lyu, R., HipSci Consortium; and Wang, W., et al. (2020). Cardelino: computational integration of somatic clonal substructure and single-cell transcriptomes. Nat. Methods *17*, 414–421.
176. La Manno, G., Soldatov, R., Zeisel, A., Braun, E., Hochgerner, H., Petukhov, V., Lidschreiber, K., Kastriti, M.E., Lönnerberg, P., Furlan, A., et al. (2018). RNA velocity of single cells. Nature *560*, 494–498.
177. Wu, F., Fan, J., He, Y., Xiong, A., Yu, J., Li, Y., Zhang, Y., Zhao, W., Zhou, F., Li, W., et al. (2021). Single-cell profiling of tumor heterogeneity and the microenvironment in advanced non-small cell lung cancer. Nat. Commun. *12*, 2540.

178. Patel, A.P., Tirosh, I., Trombetta, J.J., Shalek, A.K., Gillespie, S.M., Wakimoto, H., Cahill, D.P., Nahed, B.V., Curry, W.T., Martuza, R.L., et al. (2014). Single-cell RNA-seq highlights intratumoral heterogeneity in primary glioblastoma. Science *344*, 1396–1401.

179. Chen, K., Wang, Q., Li, M., Guo, H., Liu, W., Wang, F., Tian, X., and Yang, Y. (2021). Single-cell RNA-seq reveals dynamic change in tumor microenvironment during pancreatic ductal adenocarcinoma malignant progression. EBioMedicine *66*, 103315.

180. Zhang, Y., Narayanan, S.P., Mannan, R., Raskind, G., Wang, X., Vats, P., Su, F., Hosseini, N., Cao, X., Kumar-Sinha, C., et al. (2021). Single-cell analyses of renal cell cancers reveal insights into tumor microenvironment, cell of origin, and therapy response. Proc. Natl. Acad. Sci. USA *118*, e2103240118. https://doi.org/10.1073/pnas.2103240118.

181. Li, S., Alexander, J., Kendall, J., Andrews, P., Rose, E., Orjuela, H., Park, S., Podszus, C., Shanley, L., Ma, R., et al. (2023). High-throughput single-nucleus hybrid sequencing reveals genome-transcriptome correlations in cancer. Preprint at bioRxiv. https://doi.org/10.1101/2023.10.04.560973.

182. Foster, D.S., Januszyk, M., Delitto, D., Yost, K.E., Griffin, M., Guo, J., Guardino, N., Delitto, A.E., Chinta, M., Burcham, A.R., et al. (2022). Multiomic analysis reveals conservation of cancer-associated fibroblast phenotypes across species and tissue of origin. Cancer Cell *40*, 1392–1406.e7.

183. Asp, M., Bergenstråhle, J., and Lundeberg, J. (2020). Spatially Resolved Transcriptomes-Next Generation Tools for Tissue Exploration. Bioessays *42*, e1900221.

184. Thrane, K., Eriksson, H., Maaskola, J., Hansson, J., and Lundeberg, J. (2018). Spatially Resolved Transcriptomics Enables Dissection of Genetic Heterogeneity in Stage III Cutaneous Malignant Melanoma. Cancer Res. *78*, 5970–5979.

185. Ji, A.L., Rubin, A.J., Thrane, K., Jiang, S., Reynolds, D.L., Meyers, R.M., Guo, M.G., George, B.M., Mollbrink, A., Bergenstråhle, J., et al. (2020). Multimodal Analysis of Composition and Spatial Architecture in Human Squamous Cell Carcinoma. Cell *182*, 1661–1662.

186. Moncada, R., Barkley, D., Wagner, F., Chiodin, M., Devlin, J.C., Baron, M., Hajdu, C.H., Simeone, D.M., and Yanai, I. (2020). Integrating microarray-based spatial transcriptomics and single-cell RNA-seq reveals tissue architecture in pancreatic ductal adenocarcinomas. Nat. Biotechnol. *38*, 333–342.

187. Hirz, T., Mei, S., Sarkar, H., Kfoury, Y., Wu, S., Verhoeven, B.M., Subtelny, A.O., Zlatev, D.V., Wszolek, M.W., Salari, K., et al. (2023). Dissecting the immune suppressive human prostate tumor microenvironment via integrated single-cell and spatial transcriptomic analyses. Nat. Commun. *14*, 663.

188. Janesick, A., Shelansky, R., Gottscho, A.D., Wagner, F., Williams, S.R., Rouault, M., Beliakoff, G., Morrison, C.A., Oliveira, M.F., Sicherman, J.T., et al. (2023). High resolution mapping of the tumor microenvironment using integrated single-cell, spatial and in situ analysis. Nat. Commun. *14*, 8353.

189. Angel, T.E., Aryal, U.K., Hengel, S.M., Baker, E.S., Kelly, R.T., Robinson, E.W., and Smith, R.D. (2012). Mass spectrometry-based proteomics: existing capabilities and future directions. Chem. Soc. Rev. *41*, 3912–3928.

190. Cao, L., Huang, C., Cui Zhou, D., Hu, Y., Lih, T.M., Savage, S.R., Krug, K., Clark, D.J., Schnaubelt, M., Chen, L., et al. (2021). Proteogenomic characterization of pancreatic ductal adenocarcinoma. Cell *184*, 5031–5052.e26.

191. Herrera, J.A., Mallikarjun, V., Rosini, S., Montero, M.A., Lawless, C., Warwood, S., O'Cualain, R., Knight, D., Schwartz, M.A., and Swift, J. (2020). Laser capture microdissection coupled mass spectrometry (LCM-MS) for spatially resolved analysis of formalin-fixed and stained human lung tissues. Clin. Proteomics *17*, 24.

192. Bateman, N.W., Sun, M., Bhargava, R., Hood, B.L., Darfler, M.M., Kovatich, A.J., Hooke, J.A., Krizman, D.B., and Conrads, T.P. (2011). Differential proteomic analysis of late-stage and recurrent breast cancer from formalin-fixed paraffin-embedded tissues. J. Proteome Res. *10*, 1323–1332.

193. Grünwald, B.T., Devisme, A., Andrieux, G., Vyas, F., Aliar, K., McCloskey, C.W., Macklin, A., Jang, G.H., Denroche, R., Romero, J.M., et al. (2021). Spatially confined sub-tumor microenvironments in pancreatic cancer. Cell *184*, 5577–5592.e18.

194. Hanash, S., and Schliekelman, M. (2014). Proteomic profiling of the tumor microenvironment: recent insights and the search for biomarkers. Genome Med. *6*, 12.

195. Lai, K.K.Y., Shang, S., Lohia, N., Booth, G.C., Masse, D.J., Fausto, N., Campbell, J.S., and Beretta, L. (2011). Extracellular Matrix Dynamics in Hepatocarcinogenesis: a Comparative Proteomics Study of PDGFC Transgenic and Pten Null Mouse Models. PLoS Genet. *7*, e1002147.

196. Tian, C., Clauser, K.R., Öhlund, D., Rickelt, S., Huang, Y., Gupta, M., Mani, D.R., Carr, S.A., Tuveson, D.A., and Hynes, R.O. (2019). Proteomic analyses of ECM during pancreatic ductal adenocarcinoma progression reveal different contributions by tumor and stromal cells. Proc. Natl. Acad. Sci. USA *116*, 19609–19618.

197. Labib, M., and Kelley, S.O. (2020). Single-cell analysis targeting the proteome. Nat. Rev. Chem *4*, 143–158.

198. Li, J., Van Vranken, J.G., Pontano Vaites, L., Schweppe, D.K., Huttlin, E.L., Etienne, C., Nandhikonda, P., Viner, R., Robitaille, A.M., Thompson, A.H., et al. (2020). TMTpro reagents: a set of isobaric labeling mass tags enables simultaneous proteome-wide measurements across 16 samples. Nat. Methods *17*, 399–404.

199. Specht, H., Emmott, E., Petelski, A.A., Huffman, R.G., Perlman, D.H., Serra, M., Kharchenko, P., Koller, A., and Slavov, N. (2021). Single-cell proteomic and transcriptomic analysis of macrophage heterogeneity using SCoPE2. Genome Biol. *22*, 50.

200. Schoof, E.M., Furtwängler, B., Üresin, N., Rapin, N., Savickas, S., Gentil, C., Lechman, E., Keller, U.A.D., Dick, J.E., and Porse, B.T. (2021). Quantitative single-cell proteomics as a tool to characterize cellular hierarchies. Nat. Commun. *12*, 3341.

201. Bateman, N.W., and Conrads, T.P. (2018). Recent advances and opportunities in proteomic analyses of tumour heterogeneity. J. Pathol. *244*, 628–637.

202. Gessel, M.M., Norris, J.L., and Caprioli, R.M. (2014). MALDI imaging mass spectrometry: spatial molecular analysis to enable a new age of discovery. J. Proteomics *107*, 71–82.

203. Boyle, S.T., Mittal, P., Kaur, G., Hoffmann, P., Samuel, M.S., and Klingler-Hoffmann, M. (2020). Uncovering Tumor-Stroma Inter-relationships Using MALDI Mass Spectrometry Imaging. J. Proteome Res. *19*, 4093–4103.

204. Rujchanarong, D., Lefler, J., Saunders, J.E., Pippin, S., Spruill, L., Bethard, J.R., Ball, L.E., Mehta, A.S., Drake, R.R., Ostrowski, M.C., and Angel, P.M. (2021). Defining the Tumor Microenvironment by Integration of Immunohistochemistry and Extracellular Matrix Targeted Imaging Mass Spectrometry. Cancers *13*, 4419. https://doi.org/10.3390/cancers13174419.

205. Giordano, S., Morosi, L., Veglianese, P., Licandro, S.A., Frapolli, R., Zucchetti, M., Cappelletti, G., Falciola, L., Pifferi, V., Visentin, S., et al. (2016). 3D Mass Spectrometry Imaging Reveals a Very Heterogeneous Drug Distribution in Tumors. Sci. Rep. *6*, 37027.